Network Coded Multi–Source Cooperative Communication in BICM–OFDM Networks

Toufiqul Islam, *Student Member, IEEE*, Amir Nasri, *Member, IEEE*, Robert Schober, *Fellow, IEEE*, Ranjan K. Mallik, *Senior Member, IEEE*, and Vijay K. Bhargava, *Fellow, IEEE*

***Abstract*—In this paper, we study a cooperative diversity scheme for wireless systems employing network coding and the combination of bit–interleaved coded modulation (BICM) and orthogonal frequency division multiplexing (OFDM). The considered system comprises multiple sources, one relay, and one destination. The relay decodes the signal received from all sources and performs network coding before forwarding the signal to the destination. We propose a simple cooperative maximum-ratio combining scheme for the destination which can successfully exploit the full spatial and frequency diversity offered by the channel for arbitrary numbers of sources and arbitrary linear modulation schemes. Furthermore, we propose techniques to reduce the signaling overhead and the decoding complexity at the destination. To gain insight for system design, we derive a closed–form upper bound for the asymptotic worst–case pairwise error probability and the diversity gain of the considered network coded cooperative BICM–OFDM system. These analytical results reveal the influence of various system parameters, including the number of sources, the free distance of the code, and the frequency diversity of the involved links, on performance. Based on the derived analytical results, we develop schemes for optimal relay placement and power allocation. Simulation results corroborate the derived analytical results and confirm the effectiveness of the developed optimization framework.**

***Index Terms*—BICM, OFDM, Cooperative Diversity, Network Coding.**

I. Introduction

Early cooperative diversity schemes were mainly based on distributed repetition coding where cooperating terminals forward the information bearing message received from a single source to the destination by either amplify–and–forward (AF) or decode–and–forward (DF) operations [1]–[3]. However, the resulting increase in diversity comes at the cost of a loss in spectral efficiency. This loss can be mitigated by using distributed space–time codes [4] and/or multi–code spreading techniques [5]. In these protocols, one relay is typically limited to serve only a single source at a particular time. Hence, for large networks, these relaying schemes become increasingly bandwidth inefficient since orthogonal channels are used to forward the signals of different sources.

To overcome this bandwidth bottleneck, network coding – a technique originally conceived for routing in lossless wired networks [6] – has been applied to wireless relay networks [7], [8]. To meet the high data rate requirement of next generation cellular networks, especially for the uplink, the data streams of multiple users can be network coded at a relay and then be forwarded to the base station. Network coding over Galois fields (GFs) (referred to as GFNC) is an efficient approach to increase the throughput of multi-source cooperative diversity systems [7], [9]. Several other network coding schemes such as physical–layer network coding (PNC) for two–way relaying [10] and complex field network coding (CFNC) [11] for general multi–source cooperative networks have been proposed. However, unlike GFNC, in PNC and CFNC the relay receives the transmissions of multiple sources simultaneously, which makes time and frequency synchronization challenging. Furthermore, the relay transmit signals for PNC and CFNC do not belong to a standard signal constellation and, as a result, may suffer from high peak–to–average power ratios. The diversity gain of network coded cooperative diversity systems was analyzed in [12], [14]. However, the designs and analyses presented in [7]–[12], [14] assume frequency–flat fading channels and/or transmission without forward error correction coding which is not practical.

Bit–interleaved coded modulation combined with orthogonal frequency division multiplexing (BICM–OFDM) is a popular approach to exploit the inherent diversity offered by frequency–selective channels [15] and consequently, forms the basis of many wireless standards. Therefore, it is of both theoretical and practical interest to investigate the performance of cooperative diversity systems employing GFNC and BICM–OFDM. Two–way relaying schemes based on PNC with channel coding, BICM, and OFDM were considered in [16]/[17], [19], and [20], respectively. Recently, the performance of cooperative BICM–OFDM with AF and DF relays was studied in [21] and [22], respectively. However, the analysis and design guidelines given in [16]– [22] are not applicable to multi–source cooperative BICM–OFDM communication systems with network coding. Furthermore, in this paper, we consider the realistic case of non–ideal source–relay channels and allow the relay to forward error prone packets to the destination. A similar scenario was also considered in [13] for a network with two sources and conventional maximum ratio combining (MRC) at the destination. However, MRC may result in a loss of diversity if the relay forwards erroneous packets. On the

Manuscript received July 10, 2011; revised January 17, 2012 and April 27, 2012; accepted June 10, 2012. The review of this paper was coordinated by Prof. Ananthanarayanan Chockalingam. This work was supported in part by the International Research Chairs Initiative of the International Development Research Center of Canada under Grant RP02253 and in part by a Vanier Canada Graduate Scholarship. This work was presented in part at IEEE WCNC, Cancun, Mexico, March 2011 and in part at IEEE Globecom, Houston, TX, USA, December 2011.

Toufiqul Islam, Amir Nasri, Robert Schober, and Vijay K. Bhargava are with the Department of Electrical and Computer Engineering, The University of British Columbia, Vancouver, Canada and Ranjan K. Mallik is with the Department of Electrical Engineering, Indian Institute of Technology Delhi, India (e-mail: {toufiq,amirn,rschober,vijayb}@ece.ubc.ca; rkmallik@ee.iitd.ernet.in).

other hand, for uncoded transmission cooperative maximum ratio combining (C–MRC) was shown to achieve full diversity for uncoded DF relaying in [23] and [14].

In this paper, we consider network coded cooperative BICM–OFDM systems which comprise multiple sources, one relay, and one destination. The relay first decodes the signals received from all participating sources over orthogonal channels and then performs network coding over GF(2) at the bit level. Standard BICM–OFDM employing arbitrary M–ary modulation is adopted at the sources and the relay. The destination combines the source signals received by direct transmission and network coded transmission for decoding. For this purpose, we introduce a C–MRC bit metric, which may be viewed as an extension of the C–MRC schemes in [23] and [14] to BICM transmission. The proposed C–MRC decoding scheme is shown to achieve full diversity even in case of erroneous decisions at the relay. We also propose techniques to reduce the signaling overhead and the decoding complexity of C–MRC. We provide a mathematical framework for the analysis of the asymptotic worst–case pairwise error probability (PEP) of the proposed scheme for high signal–to–noise ratio (SNR). The PEP results reveal that the proposed scheme can extract both the spatial diversity offered by the independent transmissions from the sources and the relay and the frequency diversity of the channels. We note that the diversity gain of BICM–OFDM with network coded multi–source cooperation cannot be deduced from similar results for uncoded transmission [14] or BICM–OFDM systems with a single source [21], [22], since for BICM–OFDM with network coded multi–source cooperation the frequency diversity order of the source–destination link of one source affects the diversity gain of the other sources.

The derived asymptotic PEP upper bound is exploited for optimization of the considered network coded cooperative diversity system. In particular, relay placement is considered and is shown to lead to a non–convex polynomial programming problem which can be efficiently solved by a sum of squares method [24]. Furthermore, a power allocation problem is formulated such that fairness among the performances of the different sources is maintained and solved via geometric programming [25].

The remainder of this paper is organized as follows. In Section II, the system model is introduced and the proposed C–MRC bit metric is presented. The asymptotic PEP upper bound and the diversity gain are derived in Section III. The optimization of the considered BICM–OFDM system is discussed in Section IV. In Section V, simulation results are provided, and some conclusions are drawn in Section VI.

II. System Model

The considered system consists of K source terminals, S_j, $j \in \{1, \ldots, K\}$, one relay R, and one destination terminal D, cf. Fig. 1. In this section, we describe the processing required at S_j, $j \in \{1, \ldots, K\}$, R, and D. The adopted relaying protocol comprises two phases. In Phase 1, the sources S_j transmit their symbols to relay R and destination D over K orthogonal channels. In Phase 2, R transmits a network coded version of the K source symbols to the destination. In the following, we explain the two phase signal model and the decoding.

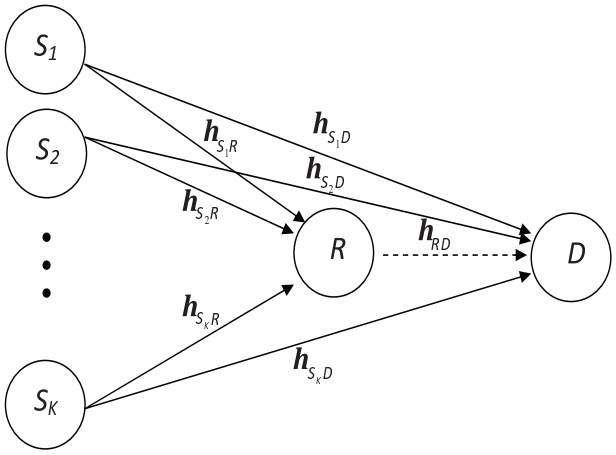

Fig. 1. Schematic block diagram of the considered cooperative diversity system. $\boldsymbol{h}_{XY}$ denotes impulse response vector of the $X \to Y$ link.

A. Phase 1

Each source S_j employs conventional BICM–OFDM [15], i.e., the output bits $c_{j,k'}$, $0 \leq k' < \log_2(M)N$, of a binary convolutional encoder with minimum free distance d_{f} are interleaved and mapped (via constellation mapping function $\mathcal{M}_x$) onto symbols $X_j[k] \in \mathcal{X}$, $k \in \mathcal{N}$, $\mathcal{N} \triangleq \{0, 1, \ldots, N-1\}$, where $\mathcal{X}$ denotes an M–ary symbol alphabet and N is the number of data sub–carriers in one OFDM symbol. The effect of the interleaver can be modeled by the mapping $k' \to (k, i)$, where k' denotes the original index of coded bit $c_{j,k'}$, and k and i denote the index of symbol $X_j[k]$ and the position of $c_{j,k'}$ in the label of $X_j[k]$, respectively. Assuming d_{f} distinct bits between any two codewords span at most d consecutive bits in the trellis, the interleaver ensures that at least every $d > d_{\mathrm{f}}$ consecutive bits at the output of the encoder are mapped to different sub–carriers [15]. The transmitted symbols are assumed to have unit average energy, i.e., $\mathcal{E}\{|X_j[k]|^2\} = 1$, where $\mathcal{E}\{\cdot\}$ denotes expectation.

Throughout this paper we assume conventional OFDM processing at the sources, the relay, and the destination and a sufficiently long cyclic prefix to avoid interference between sub–carriers. Since we assume that the sources transmit over orthogonal channels in Phase 1, the received signal at D from S_j on the kth sub–carrier can be modeled as

$$Y_{S_jD}[k] = \sqrt{P_j} H_{S_jD}[k] X_j[k] + N_{S_jD}[k], \quad \forall j, k, \qquad (1)$$

where P_j is the average transmit power in each sub–carrier at S_j, $N_{S_jD}[k]$ is complex additive white Gaussian noise (AWGN) with variance $\sigma^2_{n_{S_iD}}$, and $H_{S_jD}[k]$ is the $S_j \to D$ channel gain on sub–carrier k.

The received signal at R from S_j on the kth sub–carrier can be modeled as

$$Y_{S_jR}[k] = \sqrt{P_j} H_{S_jR}[k] X_j[k] + N_{S_jR}[k], \quad \forall j, k, \qquad (2)$$

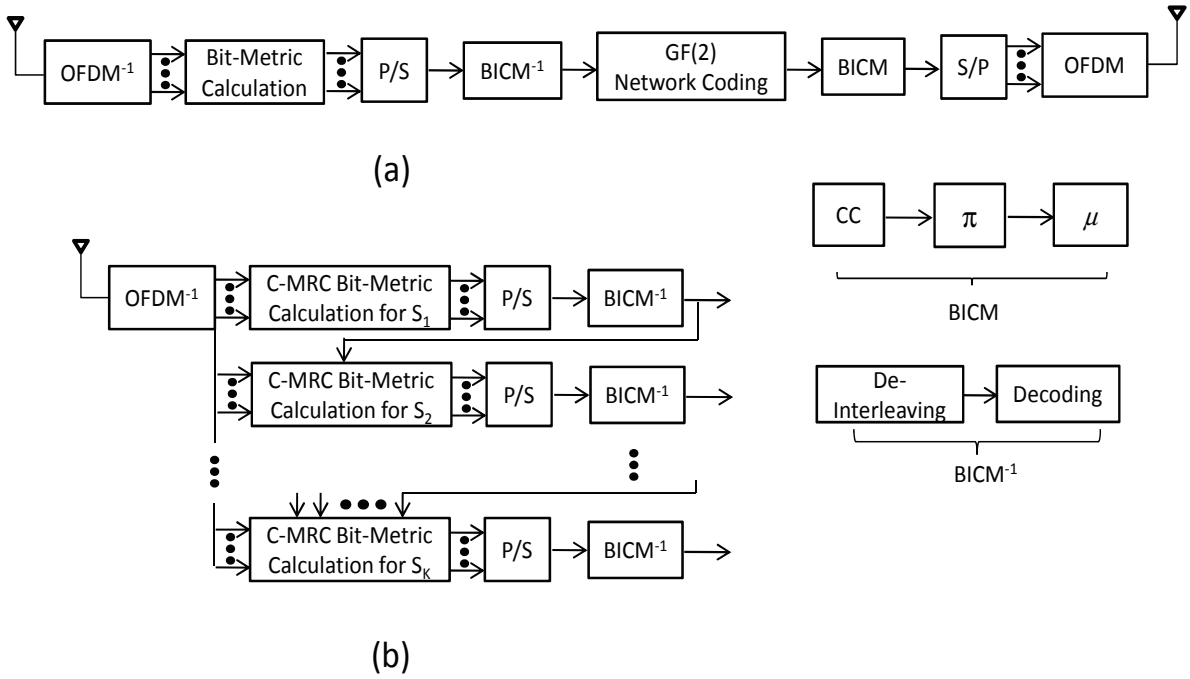

Fig. 2. Block diagram of (a) relay and (b) destination. CC: Convolutional coding; π: Bit–interleaver; and μ: Mapper.

where $N_{S_jR}[k]$ is complex AWGN with variance $\sigma^2_{n_{S_iR}}$ and $H_{S_jR}[k]$ is the $S_j \to R$ channel gain on sub–carrier k.

To decode the bits transmitted by S_j, R computes the BICM bit metric for the ith bit in the label of symbol $X_j[k]$ as [27]

$$\zeta^i_k[c_{j,k'}] = \min_{X_j \in \mathcal{X}^i_{c_{j,k'}}} \Big\{ |Y_{S_jR}[k] - \sqrt{P_j} H_{S_jR}[k] X_j|^2 \Big\}, \quad (3)$$

where $\mathcal{X}^i_b$ denotes the subset of all symbols $X \in \mathcal{X}$ whose label has value $b \in \{0, 1\}$ in position i, and in general $|\mathcal{X}^i_b| = M/2$. The bit metrics are de–interleaved and Viterbi decoded at R, cf. Fig. 2a.

B. Phase 2

In Phase 2, the relay performs GFNC at the bit level. The network coded bits are subjected to the same BICM–OFDM processing operations as the information bits at the sources. The relay transmit symbol is given by $X'_R[k] \triangleq \mathcal{M}_x\{\mathcal{M}_x^{-1}(X'_1[k]) \oplus \ldots \oplus \mathcal{M}_x^{-1}(X'_K[k])\}$, $X'_l[k] \in \{X_l[k], \hat{X}_l[k]\}$, $\forall l$, where $X'_l[k] \in \mathcal{X}$ denotes a detected symbol at R, $\hat{X}_l[k] \in \mathcal{X}$ denotes an erroneously detected symbol at R, $\mathcal{M}_x^{-1}$ denotes de–mapping, and $\oplus$ denotes addition over GF(2).

Phase 2 comprises just one time slot and the signal received at D in sub–carrier k from R is given by

$$Y_{RD}[k] = \sqrt{P_R} H_{RD}[k] X'_R[k] + N_{RD}[k], \quad k \in \mathcal{N}, \quad (4)$$

where P_R denotes the average transmit power in each sub–carrier at R, $N_{RD}[k]$ is complex AWGN with variance $\sigma^2_{n_{RD}}$, and $H_{RD}[k]$ is the frequency response of the $R \to D$ channel.

C. Decoding at Destination

We assume that the relay does not utilize an error detection mechanism (such as cyclic redundancy check (CRC) codes) and potentially forwards erroneously decoded bits. In fact, discarding packets with decoding errors at the relay is not advantageous and leads to a loss of diversity as the correctly decoded bits of the packet are lost as well. On the other hand, due to possible decision errors at the relay, conventional MRC at the destination does not achieve full diversity and optimal maximum–likelihood decoding entails a very high complexity. Therefore, we propose here a C-MRC BICM bit metric, which can be considered as an extension of the C–MRC scheme proposed in [23] and [14] for uncoded transmission and DF relaying. At D, the bit metric for source S_j for the ith bit in the label of symbol $X_j[k]$ is given by $m^i_k[c_{j,k'}]$[1]

$$= \min_{X_j \in \mathcal{X}^i_{c_{j,k'}}, X_p \in \mathcal{X}, p \neq j} \Big\{ \sum_{l=1}^{K} \frac{|Y_{S_lD}[k] - \sqrt{P_l} H_{S_lD}[k] X_l|^2}{\sigma^2_{n_{S_lD}}} + \lambda[k] \frac{|Y_{RD}[k] - \sqrt{P_R} H_{RD}[k] X'_R|^2}{\sigma^2_{n_{RD}}} \Big\}, \quad (5)$$

where X'_R is calculated by network coding from the trial source symbols X_l (cf. Section II-B) and $\lambda[k]$ is a weight factor which accounts for the relative quality of the $S_j \to R$ and $R \to D$ links. In particular, the weight $\lambda[k] \triangleq \gamma_{eq}[k]/\gamma_{RD}[k]$ accounts for the bottleneck relay link, where $\gamma_{eq}[k] \triangleq \min\{\min_j\{\gamma_{S_jR}[k]\}, \gamma_{RD}[k]\}$. Here, $\gamma_{S_jR}[k] \triangleq P_j |H_{S_jR}[k]|^2/\sigma^2_{n_{S_jR}}$ and $\gamma_{RD}[k] \triangleq P_R |H_{RD}[k]|^2/\sigma^2_{n_{RD}}$. In other words, (5) is the conventional MRC decoding metric if the $R \to D$ link is weaker than all $S_j \to R$ links (i.e., $\gamma_{S_jR}[k] \geq \gamma_{RD}[k]$, $\forall j$). If any of the $S_j \to R$ links is weaker than the $R \to D$ link, the second part of the metric in (5) is

[1]In this paper, we decode the packets of each source separately. This allows us to perform standard Viterbi decoding on the code trellises of the sources. Alternatively, the packets of all sources may be decoded jointly on a super–trellis constructed from the code trellises of all sources.

attenuated by $\lambda[k] = \min_j \gamma_{S_jR}[k]/\gamma_{RD}[k] < 1$ to limit the impact of possible decision errors at R.

D. Low Overhead C–MRC

To compute the C–MRC bit metric in (5), the destination requires knowledge of the minimum instantaneous sub–carrier gains of the $S_j \rightarrow R$ channels, $\min_j\{\gamma_{S_jR}[k]\}$, for calculation of $\lambda[k]$. The relay has to forward the estimates of $\min_j\{\gamma_{S_jR}[k]\}$ to the destination for this purpose. Depending on how fast the $S_j \rightarrow R$ links vary, this may cause a significant signaling overhead. To alleviate this problem, we propose the new weight factor

$$\lambda_r[k] \triangleq \frac{\min\{\min_j\{\bar{\gamma}_{S_jR}\}, \gamma_{RD}[k]\}}{\gamma_{RD}[k]}, \ \forall k, \qquad (6)$$

which depends on the average sub–carrier SNRs of the $S_j \rightarrow R$ links, $\bar{\gamma}_{S_jR} \triangleq P_j\sigma^2_{S_jR}/\sigma^2_{n_{S_jR}}$, $\sigma^2_{S_jR} \triangleq \mathcal{E}\{|H_{S_jR}[k]|^2\}$. In practice, $\bar{\gamma}_{S_jR}$ changes much more slowly than $\gamma_{S_jR}[k]$. As the instantaneous $\gamma_{RD}[k]$ can be directly acquired at D using training symbols, the overhead for forwarding $\min_j\{\bar{\gamma}_{S_jR}\}$ from R to D along with regular data packets is small. We refer to this scheme as low overhead C–MRC (LOC–MRC)[2].

E. Low Complexity Decoding

According to (5), the bit metric for source S_j is computed by exhausting the search space $X_l \in \mathcal{X}, \forall l, l \neq j$, which is computationally expensive for a large number of sources as it includes all possible choices of the transmit symbols of the other sources. We refer to this approach as full complexity (FC) decoding. To alleviate the computational burden, we propose a new low complexity (LC) decoding scheme. In particular, as is illustrated in Fig. 2b, in LC decoding, already decoded source symbols are exploited for decoding of the information of the other sources. Thus, LC decoding reduces the search space of the other sources' symbols for computing bit metrics for source S_j by letting $X_l = \tilde{X}_l, l \in \{1, \ldots, j-1\}, X_l \in \mathcal{X}, l \in \{j+1, \ldots, K\}$, where $\tilde{X}_l$ denotes a decoded symbol at D. For complexity comparison, we note that for (5), for each label and bit position, we have to calculate $M^K/2$ bit metrics for each source, i.e., a total of $KM^K/2$ bit metrics for all sources. On the other hand, for the proposed low complexity scheme, the number of bit metrics computed for each bit and label is given by $M^K/2 + M^{K-1}/2 + \cdots + M/2$, which results in $M(M^K-1)/(2(M-1))$ bit metrics for all sources.

For the following, we introduce the column vectors $\boldsymbol{h}_{S_jD}$, $\boldsymbol{h}_{S_jR}$, and $\boldsymbol{h}_{RD}$ containing the channel impulse response (CIR) coefficients of the $S_j \rightarrow D$, $S_j \rightarrow R$, and $R \rightarrow D$ channels, respectively. $\boldsymbol{h}_{S_jD}$, $\boldsymbol{h}_{S_jR}$, and $\boldsymbol{h}_{RD}$ are mutually independent zero–mean Gaussian random vectors (Rayleigh fading). The frequency response $H_Z[k]$, $Z \in \{S_jD, S_jR, RD\}$, can be expressed as $H_Z[k] = \boldsymbol{w}_Z^H[k]\boldsymbol{h}_Z$, where $\boldsymbol{w}_Z[k] \triangleq [1, w^k, \ldots, w^{(L_Z-1)k}]^T$ with $w \triangleq e^{j2\pi/N_t}$ (N_t: total number of sub–carriers, including both data and pilot sub–carriers) and CIR length L_Z, $Z \in \{S_jD, S_jR, RD\}$. Here, $[\cdot]^T$ and $[\cdot]^H$ denote transposition and Hermitian transposition, respectively. Note that as long as the CIR coefficients of link Z are not fully correlated, L_Z constitutes the (frequency) diversity order of the link. Furthermore, the average sub–carrier SNRs of the $S_j \rightarrow D$ and $R \rightarrow D$ links are defined as $\bar{\gamma}_{S_jD} \triangleq P_j\sigma^2_{S_jD}/\sigma^2_{n_{S_jD}}$ ($\gamma_{S_jD}[k] \triangleq P_j|H_{S_jD}[k]|^2/\sigma^2_{n_{S_jD}}$) and $\overline{\gamma}_{RD} \triangleq P_R\sigma^2_{RD}/\sigma^2_{n_{RD}}$, respectively, where $\sigma^2_U = \mathcal{E}\{|H_U[k]|^2\}$, $U \in \{S_jD, RD\}$.

[2]For computation of the LOC–MRC weight and the design problems discussed in Section V, the destination node requires knowledge of the average link SNRs. In practice, the average link SNRs can be estimated using the techniques presented in e.g. [18].

III. Performance Analysis

In this section, we derive an upper bound on the asymptotic worst–case PEP of source S_j for FC decoding with C–MRC. The main purpose of the PEP analysis is the determination of the achievable diversity gain, which provides significant insight for the design and analysis of BICM–OFDM systems [15]. Furthermore, the PEP results will also be exploited for optimal relay placement and power allocation in Section IV.

We denote the transmitted codeword by $\boldsymbol{c}_j$ and the detected codeword at the destination by $\tilde{\boldsymbol{c}}_j$. For a code with free distance d_f, $\boldsymbol{c}_j$ and $\tilde{\boldsymbol{c}}_j$ differ in d_f positions for the worst–case error event. The subset of sub–carriers containing the erroneous bits is defined as $\mathcal{K}_j \triangleq \{k_1, k_2, \cdots, k_{d_\mathrm{f}}\}$. The corresponding transmitted and detected symbols for each source are collected in vectors $\boldsymbol{x}_l \triangleq \{X_l[k]|k \in \mathcal{K}_j\}$ and $\tilde{\boldsymbol{x}}_l \triangleq \{\tilde{X}_l[k]|k \in \mathcal{K}_j\}$, respectively, where $l \in \{1, \ldots, K\}$. Note that depending on how many source symbols are received in error at R, $X'_R[k]$ defined in Section II-B may not be equal to $X_R[k]$, the relay transmit symbol when all source symbols are decoded correctly. On the other hand, multiple errors at R may cause the network coded symbol $X'_R[k]$ to equal $X_R[k]$, due to GF(2) addition at the bit level. However, taking into account multiple errors at the relay in the PEP analysis results in higher order terms which decay faster with increasing SNR compared to the cases of a single error and no error at the relay. Consequently, we assume that among the transmit symbols $X_l[k]$, $\forall l$, at most one is received in error at R. Here, $\hat{X}_{R,q}[k]$ denotes the relay transmit symbol when the signal from source S_q is received in error at R, and hence $X'_R[k]$ can be modeled as $X'_R[k] \in \{X_R[k], \hat{X}_{R,q}[k]\}$. The transmit symbols of the relay corresponding to the sub–carriers in $\mathcal{K}_j$ are collected in vector $\boldsymbol{x}'_R \triangleq \{X'_R[k]|k \in \mathcal{K}_j\}$. We also define $\boldsymbol{x} \triangleq [\boldsymbol{x}_1^T, \ldots, \boldsymbol{x}_K^T, \boldsymbol{x}_R'^T]^T$ and $\tilde{\boldsymbol{x}} \triangleq [\tilde{\boldsymbol{x}}_1^T, \ldots, \tilde{\boldsymbol{x}}_K^T, \tilde{\boldsymbol{x}}_R^T]^T$, where $\tilde{\boldsymbol{x}}_R \triangleq \{\tilde{X}_R[k]|k \in \mathcal{K}_j\}$ and $\tilde{\boldsymbol{x}}$ is the vector of the detected symbols at D. Both $\boldsymbol{x}$ and $\tilde{\boldsymbol{x}}$ contain $K+1$ vector elements, where each element itself is a $d_\mathrm{f} \times 1$ vector.

A. Asymptotic PEP

In this subsection, we analyze the worst–case PEP for C–MRC for $\overline{\gamma}_{S_lD}, \overline{\gamma}_{S_lR}, \overline{\gamma}_{RD} \rightarrow \infty$, $\forall l$. For this purpose, we first define vectors $\boldsymbol{h}_{SD} \triangleq [\boldsymbol{h}_{S_1D}^T, \ldots, \boldsymbol{h}_{S_KD}^T]^T$, $\boldsymbol{h}_{SR} \triangleq [\boldsymbol{h}_{S_1R}^T, \ldots, \boldsymbol{h}_{S_KR}^T]^T$, and $\boldsymbol{h} \triangleq [\boldsymbol{h}_{SD}^T, \boldsymbol{h}_{SR}^T, \boldsymbol{h}_{RD}^T]^T$. Assuming a code with free distance d_f, the worst–case PEP of two codewords $\boldsymbol{c}_j$ and $\tilde{\boldsymbol{c}}_j$ can be bounded as

$$P(\boldsymbol{c}_j, \tilde{\boldsymbol{c}}_j) \leq P_1(\boldsymbol{c}_j, \tilde{\boldsymbol{c}}_j) + P_2(\boldsymbol{c}_j, \tilde{\boldsymbol{c}}_j), \qquad (7)$$

$$P_D(\boldsymbol{c}_j,\,\tilde{\boldsymbol{c}}_j|\boldsymbol{h},\boldsymbol{x}_R)=\Pr\Bigg\{\sum_{k\in\mathcal{K}_j}m_k^i[c_{j,k'}]\geq\sum_{k\in\mathcal{K}_j}m_k^i[\tilde{c}_{j,k'}]\Bigg\}$$
$$=\Pr\Bigg\{\sum_{k\in\mathcal{K}_j}\Bigg(\sum_{l=1}^{K}\gamma_{S_lD}[k]|X_l[k]-\tilde{X}_l[k]|^2+\gamma_{eq}[k]|X_R[k]-\tilde{X}_R[k]|^2+\sum_{l=1}^{K}\frac{2\Re\{\sqrt{P_l}H_{S_lD}[k](X_l[k]-\tilde{X}_l[k])N^*_{S_lD}[k]\}}{\sigma^2_{n_{S_lD}}}$$
$$+\lambda[k]\frac{2\Re\{\sqrt{P_R}H_{RD}[k](X_R[k]-\tilde{X}_R[k])N^*_{RD}[k]\}}{\sigma^2_{n_{RD}}}\Bigg)\leq 0\Bigg\}=\Pr\{\mu+z\leq 0\},\tag{10}$$

$$P_D(\boldsymbol{c}_j,\,\tilde{\boldsymbol{c}}_j|\boldsymbol{h},\hat{\boldsymbol{x}}_{R,q})=\Pr\Bigg\{\sum_{k\in\mathcal{K}_j}\Bigg(\sum_{l=1}^{K}\gamma_{S_lD}[k]|X_l[k]-\tilde{X}_l[k]|^2+\gamma_{eq}[k](|\hat{X}_{R,q}[k]-\tilde{X}_R[k]|^2-|\hat{X}_{R,q}[k]-X_R[k]|^2)$$
$$+\sum_{l=1}^{K}\frac{2\Re\{\sqrt{P_l}H_{S_lD}[k](X_l[k]-\tilde{X}_l[k])N^*_{S_lD}[k]\}}{\sigma^2_{n_{S_lD}}}+\lambda[k]\frac{2\Re\{\sqrt{P_R}H_{RD}[k](X_R[k]-\tilde{X}_R[k])N^*_{RD}[k]\}}{\sigma^2_{n_{RD}}}\Bigg)\leq 0\Bigg\}=\Pr\{\nu+s\leq 0\},\tag{13}$$

where $P_1(\boldsymbol{c}_j,\,\tilde{\boldsymbol{c}}_j)$ and $P_2(\boldsymbol{c}_j,\,\tilde{\boldsymbol{c}}_j)$ denote the PEPs for correct and erroneous re-transmission at the relay, respectively, and are given by

$$P_1(\boldsymbol{c}_j,\,\tilde{\boldsymbol{c}}_j)\triangleq\mathcal{E}_{\boldsymbol{h}}\Big\{P_D(\boldsymbol{c}_j,\,\tilde{\boldsymbol{c}}_j|\boldsymbol{h},\boldsymbol{x}_R)\Big\},\tag{8}$$

$$P_2(\boldsymbol{c}_j,\,\tilde{\boldsymbol{c}}_j)\triangleq\mathcal{E}_{\boldsymbol{h}}\Big\{\sum_{q=1}^{K}P_R(\boldsymbol{c}_q,\,\hat{\boldsymbol{c}}_q|\boldsymbol{h}_{S_qR})P_D(\boldsymbol{c}_j,\,\tilde{\boldsymbol{c}}_j|\boldsymbol{h},\hat{\boldsymbol{x}}_{R,q})\Big\}.\tag{9}$$

Here, $P_1(\boldsymbol{c}_j,\tilde{\boldsymbol{c}}_j)$ is an upper bound as the probability of correct detection at the relay is ignored (which also makes the right hand side of (7) an upper bound), $\boldsymbol{x}_R\triangleq\{X_R[k]|k\in\mathcal{K}_j\}$, $\hat{\boldsymbol{x}}_{R,q}\triangleq\{\hat{X}_{R,q}[k]|k\in\mathcal{K}_j\}$, $P_R(\boldsymbol{c}_q,\,\hat{\boldsymbol{c}}_q|\boldsymbol{h}_{S_qR})$ denotes the worst–case PEP at the relay if the signal of source S_q is received in error at R, $P_D(\boldsymbol{c}_j,\,\tilde{\boldsymbol{c}}_j|\boldsymbol{h},\boldsymbol{x}_R)$ denotes the PEP at the destination when there is no decoding error at R, and $P_D(\boldsymbol{c}_j,\,\tilde{\boldsymbol{c}}_j|\boldsymbol{h},\hat{\boldsymbol{x}}_{R,q})$ denotes the PEP at the destination when the relay transmit symbol is erroneous due to a decoding error of the signal received from source S_q at R.

When there is no decoding error at R, based on (5) the worst–case PEP of source S_j at the destination conditioned on $\boldsymbol{h}$ can be expressed as shown in (10) at the top of this page, where $\Re\{\cdot\}$ denotes the real part of a complex number, $\mu\triangleq\sum_{k\in\mathcal{K}_j}(\sum_{l=1}^{K}\gamma_{S_lD}[k]d_l^2[k]+\gamma_{eq}[k]d_R^2[k])$, and z is an AWGN term with variance $\sigma_z^2\triangleq 2\sum_{k\in\mathcal{K}_j}(\sum_{l=1}^{K}\gamma_{S_lD}[k]d_l^2[k]+\gamma_{eq}^2[k]d_R^2[k]/\gamma_{RD}[k])$. Here, $d_l^2[k]\triangleq|X_l[k]-\tilde{X}_l[k]|^2$, $d_R^2[k]\triangleq|X_R[k]-\tilde{X}_R[k]|^2$, and we exploited the definition of $\lambda[k]$. Using the Chernoff bound on the Gaussian Q–function and exploiting the fact that $\gamma_{eq}[k]\leq\gamma_{RD}[k]$, we obtain from (10)

$$P_D(\boldsymbol{c}_j,\,\tilde{\boldsymbol{c}}_j|\boldsymbol{h},\boldsymbol{x}_R)$$
$$\leq\frac{1}{2}\exp\Big(-\frac{1}{4}\sum_{k\in\mathcal{K}_j}\big(\sum_{l=1}^{K}\gamma_{S_lD}[k]d_l^2[k]+\gamma_{eq}[k]d_R^2[k]\big)\Big).\tag{11}$$

If the signal from source S_q is received in error at R, then the conditional PEP at R can be upper–bounded as [15]

$$P_R(\boldsymbol{c}_q,\,\hat{\boldsymbol{c}}_q|\boldsymbol{h}_{S_qR})\leq\frac{1}{2}\exp\Big(-\frac{1}{4}\sum_{k\in\mathcal{K}_j}\gamma_{S_qR}[k]\hat{d}_q^2[k]\Big),\tag{12}$$

where $\hat{d}_q^2[k]\triangleq|X_q[k]-\hat{X}_q[k]|^2$. Furthermore, if there is a decoding error at R, based on (5) the worst–case PEP for source S_j at D conditioned on $\boldsymbol{h}$ can be expressed as shown in (13) at the top of this page, where $\nu\triangleq\sum_{k\in\mathcal{K}_j}(\sum_{l=1}^{K}\gamma_{S_lD}[k]d_l^2[k]+\gamma_{eq}[k]\hat{d}_{R,q}^2[k])$, s is an AWGN term with variance $\sigma_s^2\triangleq 2\sum_{k\in\mathcal{K}_j}(\sum_{l=1}^{K}\gamma_{S_lD}[k]d_l^2[k]+\gamma_{eq}^2[k]d_R^2[k]/\gamma_{RD}[k])$, and $\hat{d}_{R,q}^2[k]\triangleq|\hat{X}_{R,q}[k]-\tilde{X}_R[k]|^2-|\hat{X}_{R,q}[k]-X_R[k]|^2$. Employing the Chernoff bound and the fact that $\gamma_{eq}[k]\leq\gamma_{RD}[k]$, we have

$$P_D(\boldsymbol{c}_j,\,\tilde{\boldsymbol{c}}_j|\boldsymbol{h},\hat{\boldsymbol{x}}_{R,q})$$
$$\leq\frac{1}{2}\exp\Bigg(-\frac{\big(\sum_{k\in\mathcal{K}_j}\big(\sum_{l=1}^{K}\gamma_{S_lD}[k]d_l^2[k]+\gamma_{eq}[k]\hat{d}_{R,q}^2[k]\big)\big)^2}{4\sum_{k\in\mathcal{K}_j}\big(\sum_{l=1}^{K}\gamma_{S_lD}[k]d_l^2[k]+\gamma_{eq}[k]d_R^2[k]\big)}\Bigg).\tag{14}$$

In the following, we consider the error events which yield the lowest possible diversity order at high SNR. Let $d_H(\boldsymbol{x},\tilde{\boldsymbol{x}})$ denotes the number of symbols in which $\boldsymbol{x}$ and $\tilde{\boldsymbol{x}}$ differ. We study the cases when $\boldsymbol{x}$ and $\tilde{\boldsymbol{x}}$ differ in the minimum possible number of vector elements (two in this case), where each vector element consists of d_{f} symbols. So, for all possible pairs, we have $d_H(\boldsymbol{x},\tilde{\boldsymbol{x}})\geq 2d_{\mathrm{f}}$. Since error events with $d_H(\boldsymbol{x},\tilde{\boldsymbol{x}})>2d_{\mathrm{f}}$ yield a higher diversity gain than error events with $d_H(\boldsymbol{x},\tilde{\boldsymbol{x}})=2d_{\mathrm{f}}$, their contribution to the asymptotic PEP is negligible. Thus, we focus on the two types of error events (Cases 1 and 2) with $d_H(\boldsymbol{x},\tilde{\boldsymbol{x}})=2d_{\mathrm{f}}$. We evaluate the conditional probabilities in (11), (12), and (14) for these two cases to obtain $P_1^n(\boldsymbol{c}_j,\,\tilde{\boldsymbol{c}}_j)$ and $P_2^n(\boldsymbol{c}_j,\,\tilde{\boldsymbol{c}}_j)$ in (8) and (9), where $n\in\{1,2\}$ refers to the case under study.

Case 1: As $\boldsymbol{c}_j$ and $\tilde{\boldsymbol{c}}_j$ differ in d_{f} bits and are mapped to $\boldsymbol{x}_j$ and $\tilde{\boldsymbol{x}}_j$, respectively, we have $\boldsymbol{x}_j\neq\tilde{\boldsymbol{x}}_j$. For Case 1, we assume $\boldsymbol{x}_l=\tilde{\boldsymbol{x}}_l$, $l\in\{1,\ldots,K\}$, $l\neq j$, and $\boldsymbol{x}'_R\neq\tilde{\boldsymbol{x}}_R$. Thus, we observe that $\boldsymbol{x}$ and $\tilde{\boldsymbol{x}}$ differ in two vector elements, i.e., in a total of $2d_{\mathrm{f}}$ positions as each vector element is of size d_{f}, cf. Fig. 3, Case 1. Here, we get $d_l[k]=0$, $\forall l$, $l\neq j$, and obtain from (11) as $P_D(\boldsymbol{c}_j,\,\tilde{\boldsymbol{c}}_j|\boldsymbol{h},\boldsymbol{x}_R)$

$$\leq\frac{1}{2}\exp\Big(-\frac{1}{4}\sum_{k\in\mathcal{K}_j}\big(\gamma_{S_jD}[k]d_j^2[k]+\gamma_{eq}[k]d_R^2[k]\big)\Big)$$

$$\leq \frac{1}{2}\exp\Big(-\xi(\gamma_{s,j}+\gamma_m)\Big), \tag{15}$$

where $\gamma_{s,j} \triangleq \sum_{k\in\mathcal{K}_j}\gamma_{S_jD}[k]$, $\gamma_m \triangleq \sum_{k\in\mathcal{K}_j}\gamma_{eq}[k]$, $\xi \triangleq d_{\min}^2/4$, and we have replaced $d_j[k]$ and $d_R[k]$ by $d_{\min}$ (minimum Euclidean distance of signal constellation $\mathcal{X}$), which corresponds to a further upper bounding. Since $\gamma_{eq}[k] = \min\{\{\min_l \gamma_{S_lR}[k]\}, \gamma_{RD}[k]\} \geq \frac{1}{\sum_l \frac{1}{\gamma_{S_lR}[k]}+\frac{1}{\gamma_{RD}[k]}}$, we obtain from (8) and (15) an upper bound for the unconditional PEP assuming no error at R for Case 1 as [21, Eq. (18)]

$$P_1^1(\boldsymbol{c}_j, \tilde{\boldsymbol{c}}_j) \leq \frac{1}{2}\frac{1}{(\xi\bar{\gamma}_{S_jD})^{r_{S_jD}}\prod_{m=1}^{r_{S_jD}}\lambda_m(\boldsymbol{W}_{S_jD}\boldsymbol{C}_{S_jD})} \times\Bigg[\sum_{l=1}^{K}\frac{1}{(\xi\bar{\gamma}_{S_lR})^{r_{S_lR}}\prod_{m=1}^{r_{S_lR}}\lambda_m(\boldsymbol{W}_{S_lR}\boldsymbol{C}_{S_lR})} +\frac{1}{(\xi\bar{\gamma}_{RD})^{r_{RD}}\prod_{m=1}^{r_{RD}}\lambda_m(\boldsymbol{W}_{RD}\boldsymbol{C}_{RD})}\Bigg], \tag{16}$$

where $\lambda_m(\boldsymbol{X})$ denotes the non–zero eigenvalues of matrix $\boldsymbol{X}$ and $r_Z \triangleq \text{rank}\{\boldsymbol{W}_Z\boldsymbol{C}_Z\} = \min\{d_{\text{f}}, L_Z\}$, $Z \in \{S_jD, S_jR, RD\}$. Here, $\boldsymbol{W}_Z \triangleq \sum_{k,d_{\text{f}}}\boldsymbol{w}_Z[k]\boldsymbol{w}_Z^H[k]$ is a sub–carrier dependent matrix and $\boldsymbol{C}_Z$ is the correlation matrix of $\boldsymbol{h}_Z$, which is assumed to have full rank for all $Z \in \{S_jD, S_jR, RD\}$.

Similarly, from (14), we obtain for Case 1

$$P_D(\boldsymbol{c}_j, \tilde{\boldsymbol{c}}_j|\boldsymbol{h}, \hat{\boldsymbol{x}}_{R,q}) \leq \frac{1}{2}\exp\left(-\xi\frac{(\sum_{k\in\mathcal{K}_j}(\gamma_{S_jD}[k]-\beta\gamma_{eq}[k]))^2}{\sum_{k\in\mathcal{K}_j}(\gamma_{S_jD}[k]+\gamma_{eq}[k])}\right), \tag{17}$$

where we have used $\hat{d}_{R,q}^2[k] = |\hat{X}_{R,q}[k]-\tilde{X}_R[k]|^2 - |\hat{X}_{R,q}[k]-X_R[k]|^2 \geq -\beta d_{\min}^2$ to arrive at an upper bound. Here, $\beta \triangleq 1$ for $M = 2$ (BPSK) and $\beta \triangleq \chi^2 - 1$ for $M > 2$, and $\chi \triangleq d_{\max}/d_{\min}$ ($\chi > 1$) holds, where $d_{\max}$ denotes the maximum Euclidean distance of signal constellation $\mathcal{X}$. For the following, we use the definitions of $\gamma_{s,j}$ and γ_m in (17), which leads to

$$P_D(\boldsymbol{c}_j, \tilde{\boldsymbol{c}}_j|\boldsymbol{h}, \hat{\boldsymbol{x}}_{R,q}) \leq \frac{1}{2}\exp\left(-\xi\frac{(\gamma_{s,j}-\beta\gamma_m)^2}{\gamma_{s,j}+\gamma_m}\right). \tag{18}$$

Furthermore, replacing $\hat{d}_q[k]$ by $d_{\min}$ and using $\gamma_{S_qR} \triangleq \sum_{k\in\mathcal{K}_j}\gamma_{S_qR}[k]$ in (12), we obtain the conditional PEP at R as

$$P_R(\boldsymbol{c}_q, \hat{\boldsymbol{c}}_q|\boldsymbol{h}_{S_qR}) \leq \frac{1}{2}\exp\left(-\xi\gamma_{S_qR}\right). \tag{19}$$

Thus, based on (8), (18), and (19), the unconditional PEP assuming a detection error at R for Case 1 can be expressed as $P_2^1(\boldsymbol{c}_j, \tilde{\boldsymbol{c}}_j)$

$$\leq \frac{1}{4}\mathcal{E}_{\boldsymbol{h}}\left\{\sum_{q=1}^{K}\exp(-\xi\gamma_{S_qR})\exp\left(-\xi\frac{(\gamma_{s,j}-\beta\gamma_m)^2}{\gamma_{s,j}+\gamma_m}\right)\right\}. \tag{20}$$

Since $\gamma_m \leq \min\{\gamma_{S_lR}, \gamma_{RD}\} \leq \gamma_{S_lR}$ with $\gamma_{RD} \triangleq \sum_{k\in\mathcal{K}_j}\gamma_{RD}[k]$ is valid, $P_2^1(\boldsymbol{c}_j, \tilde{\boldsymbol{c}}_j)$ can be further upper bounded as

$$P_2^1(\boldsymbol{c}_j, \tilde{\boldsymbol{c}}_j) \leq \frac{1}{4}\sum_{q=1}^{K}\mathcal{E}_{\boldsymbol{h}}\left\{\exp\left(-\xi\left(\gamma_m+\frac{(\gamma_{s,j}-\beta\gamma_m)^2}{\gamma_{s,j}+\gamma_m}\right)\right)\right\}$$

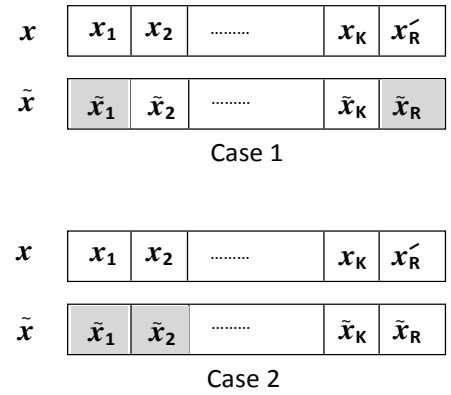

Fig. 3. Example illustrating the Cases 1 and 2 considered for the PEP analysis in Section III. $j = 1$ and $p = 2$ are valid. The shaded elements in $\tilde{\boldsymbol{x}}$ denote the elements that do not agree with the corresponding elements in $\boldsymbol{x}$.

$$= K(\text{I}_1 + \text{I}_2), \tag{21}$$

with[3]

$$\text{I}_1 \leq \frac{1}{4}\mathcal{E}_{\boldsymbol{h}_{S_jD}}\left\{\exp\Big(-\xi\varphi\sum_{k\in\mathcal{K}}\gamma_{S_jD}[k]\Big)\right\} \times\mathcal{E}_{\boldsymbol{h}_{SR},\boldsymbol{h}_{RD}}\left\{\exp\Big(-\xi\varphi\sum_{k\in\mathcal{K}}\gamma_{eq}[k]\Big)\right\} \tag{22}$$

$$\text{I}_2 \leq \frac{1}{4}\mathcal{E}_{\boldsymbol{h}_{S_jD}}\left\{\exp\Big(-\xi\sum_{k\in\mathcal{K}}\gamma_{S_jD}[k]\Big)\right\} \times\mathcal{E}_{\boldsymbol{h}_{SR},\boldsymbol{h}_{RD}}\left\{\exp\Big(-\xi\sum_{k\in\mathcal{K}}\gamma_{eq}[k]\Big)\right\}, \tag{23}$$

where $\varphi = \rho\beta^2/(1+\beta)^2 > 0$ is a modulation dependent parameter and ρ is given by

$$\rho = -\frac{3+2\beta+\beta^2}{2} + \frac{3+2\beta+\beta^2}{2}\sqrt{1+\frac{4(4\beta+3)}{3+2\beta+\beta^2}}. \tag{24}$$

Combining I_1 and I_2 and exploiting again [21, Eq. (18)], we obtain from (21)

$$P_2^1(\boldsymbol{c}_j, \tilde{\boldsymbol{c}}_j) \leq \frac{1}{4}\frac{K}{(\xi\bar{\gamma}_{S_jD})^{r_{S_jD}}\prod_{m=1}^{r_{S_jD}}\lambda_m(\boldsymbol{W}_{S_jD}\boldsymbol{C}_{S_jD})} \Bigg[\sum_{l=1}^{K}\left(1+\frac{1}{\varphi^{r_{S_jD}+r_{S_lR}}}\right)\frac{1}{(\xi\bar{\gamma}_{S_lR})^{r_{S_lR}}\prod_{m=1}^{r_{S_lR}}\lambda_m(\boldsymbol{W}_{S_lR}\boldsymbol{C}_{S_lR})} +\left(1+\frac{1}{\varphi^{r_{S_jD}+r_{RD}}}\right)\frac{1}{(\xi\bar{\gamma}_{RD})^{r_{RD}}\prod_{m=1}^{r_{RD}}\lambda_m(\boldsymbol{W}_{RD}\boldsymbol{C}_{RD})}\Bigg]. \tag{25}$$

Case 2: Assuming $\boldsymbol{x}'_R = \tilde{\boldsymbol{x}}_R$ and $\boldsymbol{x}_l \neq \tilde{\boldsymbol{x}}_l$, $l \in \{j, p\}$, $p \in \{1, \ldots, K\}$, $p \neq j$, and $\boldsymbol{x}_l = \tilde{\boldsymbol{x}}_l$, otherwise, also causes $\boldsymbol{x}$ and $\tilde{\boldsymbol{x}}$ to differ in two vector elements and we obtain $d_H(\boldsymbol{x}, \tilde{\boldsymbol{x}}) = 2d_{\text{f}}$, cf. Fig. 3, Case 2. It is possible that in Case 2, $\boldsymbol{x}_p$ and $\tilde{\boldsymbol{x}}_p$ do not differ in all d_{f} positions. Depending on the start of the error event, the set of sub–carriers containing the erroneous bits corresponding to $\boldsymbol{x}_p$ and $\tilde{\boldsymbol{x}}_p$ may only partially overlap

[3]A detailed proof is given in the conference version in [22, Eqs. (18–27)] but omitted here because of space constraints.

$$P(\boldsymbol{c}_j,\,\tilde{\boldsymbol{c}}_j) \le \frac{1}{(\xi\bar{\gamma}_{S_jD})^{r_{S_jD}}\prod_{m=1}^{r_{S_jD}}\lambda_m(\boldsymbol{W}_{S_jD}\boldsymbol{C}_{S_jD})}\left[\sum_{l=1}^{K}\frac{\theta_{l,R}^{j}}{(\xi\bar{\gamma}_{S_lR})^{r_{S_lR}}\prod_{m=1}^{r_{S_lR}}\lambda_m(\boldsymbol{W}_{S_lR}\boldsymbol{C}_{S_lR})}\right.$$
$$\left.+\sum_{p=1,p\neq j}^{K}\frac{\theta_{p,D}}{(\xi\bar{\gamma}_{S_pD})^{r_{S_pD}}\prod_{m=1}^{r_{S_pD}}\lambda_m(\boldsymbol{W}_{S_pD}\boldsymbol{C}_{S_pD})}+\frac{\theta_{RD}^{j}}{(\xi\bar{\gamma}_{RD})^{r_{RD}}\prod_{m=1}^{r_{RD}}\lambda_m(\boldsymbol{W}_{RD}\boldsymbol{C}_{RD})}\right] \tag{32}$$

with $\mathcal{K}_j$. However, the cases with a partial overlap yield higher diversity gains, and hence can be omitted at high SNR. So, to obtain a simple upper bound on the worst–case PEP at D for Case 2, we assume that all elements in $\boldsymbol{x}_p$ differ from $\tilde{\boldsymbol{x}}_p$. We obtain from (11) for Case 2

$$P_D(\boldsymbol{c}_j,\,\tilde{\boldsymbol{c}}_j|\boldsymbol{h},\boldsymbol{x}_R) \le \frac{1}{2}\exp\Big(-\frac{1}{4}\sum_{k\in\mathcal{K}_j}\sum_{l\in\{j,p\}}\gamma_{S_lD}[k]d_l^2[k]\Big), \tag{26}$$

since $d_R[k]=0$. Using the same upper–bounding techniques as adopted in (16), we obtain an upper bound for the unconditional PEP assuming no error at R as

$$P_1^2(\boldsymbol{c}_j,\,\tilde{\boldsymbol{c}}_j) \le \frac{1}{4}\frac{1}{(\xi\bar{\gamma}_{S_jD})^{r_{S_jD}}\prod_{m=1}^{r_{S_jD}}\lambda_m(\boldsymbol{W}_{S_jD}\boldsymbol{C}_{S_jD})}$$
$$\times\left(\sum_{p=1,\ p\neq j}^{K}\frac{1}{(\xi\bar{\gamma}_{S_pD})^{r_{S_pD}}\prod_{m=1}^{r_{S_pD}}\lambda_m(\boldsymbol{W}_{S_pD}\boldsymbol{C}_{S_pD})}\right). \tag{27}$$

For the case when the symbol from source S_q is received in error at R, we obtain for Case 2 from (14)

$$\begin{aligned}&P_D(\boldsymbol{c}_j,\,\tilde{\boldsymbol{c}}_j|\boldsymbol{h},\hat{\boldsymbol{x}}_{R,q})\\ &\le\frac{1}{2}\exp\Big(-\frac{1}{4}\frac{\big(\sum_{k\in\mathcal{K}_j}\sum_{l\in\{j,p\}}\gamma_{S_lD}[k]d_l^2[k]\big)^2}{\sum_{k\in\mathcal{K}_j}\sum_{l\in\{j,p\}}\gamma_{S_lD}[k]d_l^2[k]}\Big)\\ &=\frac{1}{2}\exp\Big(-\xi\sum_{l\in\{j,p\}}\sum_{k\in\mathcal{K}_j}\gamma_{S_lD}[k]\Big),\end{aligned} \tag{28}$$

since $\hat{d}_{R,q}^2[k]=0$ and $d_R[k]=0$, as $\boldsymbol{x}_R=\tilde{\boldsymbol{x}}_R$. From (28), we have

$$P_D(\boldsymbol{c}_j,\,\tilde{\boldsymbol{c}}_j|\boldsymbol{h},\hat{\boldsymbol{x}}_{R,q}) \le \frac{1}{2}\exp(-\xi(\gamma_{s,j}+\gamma_{s,p})). \tag{29}$$

Following (8), (19), and (29) and for $p\in\{1,\ldots,K\},\ p\neq j$, we obtain the following upper bound on the unconditional PEP assuming an error at R for Case 2

$$\begin{aligned}P_2^2(\boldsymbol{c}_j,\,\tilde{\boldsymbol{c}}_j) &\le\frac{1}{4}\mathcal{E}_{\boldsymbol{h}}\Big\{\sum_{p=1,p\neq j}^{K}\sum_{q=1}^{K}\exp(-\xi(\gamma_{S_qR}+\gamma_{s,j}+\gamma_{s,p}))\Big\}\\ &\le\frac{1}{4}\mathcal{E}_{\boldsymbol{h}}\Big\{\sum_{p=1,p\neq j}^{K}\sum_{q=1}^{K}\exp(-\xi(\gamma_{m}+\gamma_{s,j}+\gamma_{s,p}))\Big\},\\ &=\frac{K}{4}\mathcal{E}_{\boldsymbol{h}}\Big\{\exp(-\xi(\gamma_m+\gamma_{s,j}))\sum_{p=1,p\neq j}^{K}\exp(-\xi\gamma_{s,p})\Big\},\end{aligned} \tag{30}$$

since $\gamma_m \le \min\{\gamma_{S_qR},\gamma_{RD}\} \le \gamma_{S_qR}$ is valid. Following similar steps as adopted to arrive at (16), evaluation of (30) leads to

$$P_2^2(\boldsymbol{c}_j,\,\tilde{\boldsymbol{c}}_j) \le \frac{K}{4}\frac{1}{(\xi\bar{\gamma}_{S_jD})^{r_{S_jD}}\prod_{m=1}^{r_{S_jD}}\lambda_m(\boldsymbol{W}_{S_jD}\boldsymbol{C}_{S_jD})}$$
$$\times\left(\sum_{l=1}^{K}\frac{1}{(\xi\bar{\gamma}_{S_lR})^{r_{S_lR}}\prod_{m=1}^{r_{S_lR}}\lambda_m(\boldsymbol{W}_{S_lR}\boldsymbol{C}_{S_lR})}\right.$$
$$\left.+\frac{1}{(\xi\bar{\gamma}_{RD})^{r_{RD}}\prod_{m=1}^{r_{RD}}\lambda_m(\boldsymbol{W}_{RD}\boldsymbol{C}_{RD})}\right)$$
$$\times\sum_{p=1\ (p\neq j)}^{K}\frac{1}{(\xi\bar{\gamma}_{S_pD})^{r_{S_pD}}\prod_{m=1}^{r_{S_pD}}\lambda_m(\boldsymbol{W}_{S_pD}\boldsymbol{C}_{S_pD})}. \tag{31}$$

A careful investigation of (31) reveals that the right hand side of (31) decays faster than the right hand sides of (16), (25), and (27) at high SNR, and consequently is not relevant for the final asymptotic PEP upper bound.

Combining (16), (25), and (27) we obtain an upper bound for the PEP at the destination in (32) at the top of this page, where

$$\begin{aligned}\theta_{l,R}^{j}&\triangleq\frac{1}{2}+\frac{K}{4}\Big(1+\frac{1}{\varphi^{r_{S_jD}+r_{S_lR}}}\Big),\\ \theta_{RD}^{j}&\triangleq\frac{1}{2}+\frac{K}{4}\Big(1+\frac{1}{\varphi^{r_{S_jD}+r_{RD}}}\Big),\ \text{and}\ \theta_{p,D}\triangleq\frac{1}{4}.\end{aligned} \tag{33}$$

From (32), we observe that the PEP increases with increasing number of sources. Hence, the error rate performance of the considered multi–source system may be worse than that of cooperative BICM–OFDM systems employing AF and DF relaying [21], [22]. However, this loss is more than compensated by the throughput gain offered by the network coded system, which requires only $K+1$ time slots for transmitting K source signals, whereas conventional AF and DF relaying require $2K$ time slots.

B. Diversity Gain

To get more insight into the system performance, we investigate the diversity gain. Letting $\overline{\gamma}_{S_lD}=e_l\overline{\gamma}_t$, $\overline{\gamma}_{S_lR}=f_l\overline{\gamma}_t$, and $\overline{\gamma}_{RD}=g\overline{\gamma}_t$, $\forall l$, where e_l, f_l, and g are arbitrary positive constants, we define the diversity gain as the negative slope of the PEP in (32) as a function of $\overline{\gamma}_t$ on a double–logarithmic scale. Thus, based on (32), the diversity gain for source S_j is given by

$$\begin{aligned}G_d^j&=r_{S_jD}+\min\{\min_l\{r_{S_lR}\},\ \min_{p,\ p\neq j}\{r_{S_pD}\},r_{RD}\}\\ &=\min\{d_{\mathrm{f}},L_{S_jD}\}+\min\{d_{\mathrm{f}},\min_l\{L_{S_lR}\},\min_{p,\ p\neq j}\{L_{S_pD}\},L_{RD}\}.\end{aligned} \tag{34}$$

Eq. (34) reveals that for source S_j, the maximum diversity gain of network coded BICM–OFDM is limited by the free distance of the code, the frequency diversity (i.e., length of

CIRs) offered by all channels, or both. We can extract the full frequency diversity offered by the channel by employing a code with sufficiently large free distance $d_{\rm f}$. For channels that are rich in frequency diversity, i.e., $L_{S_jD} \geq d_{\rm f}$ and $\min\{\min_l\{L_{S_lR}\}, \min_{p,\ p\neq j}\{L_{S_pD}\}, L_{RD}\} \geq d_{\rm f}$, we obtain $G_d = 2d_{\rm f}$ which is identical to the maximum diversity gain achievable in cooperative AF [21] and DF [22] BICM–OFDM systems. Note that different sources may enjoy different levels of diversity gain depending on the quality of the channel links. From (34), it is interesting to observe that the overall diversity gain of source S_j depends on the frequency diversity of the direct links of the other sources, which is different from conventional AF and DF cooperative BICM–OFDM systems. If the other $S_l \to D$, $l \neq j$, links are poor compared to the $S_l \to R$ and $R \to D$ links, it becomes difficult to decode the signal of source S_j at D based on the coded information received from R and direct transmissions from other sources. Hence, the error rate performance of source S_j degrades, which is evident from (34). Moreover, as decoding errors at R have been taken into account in the analysis and R forwards the coded information of all sources, the diversity gain depends on the worst $S_l \to R$, $\forall l$, link as well.

IV. Design of Network Coded BICM–OFDM Systems

In this section, we exploit the analytical results from Section III for the design and optimization of network coded cooperative BICM–OFDM systems. In particular, our goal is to optimize relay placement and power allocation for minimization of the BER or the frame error rate (FER) of the system. Since analytical expressions for the BER and FER are not available, we adopt the upper bound on the asymptotic worst–case PEP of CMRC in (32) to formulate the relevant optimization problems. The simulation results in Section V confirm that the optimization based on the upper bound on the asymptotic worstcase PEP has the intended effect on the BER and FER, cf. Figs. 8 and 9. Unfortunately, the PEP in (32) depends on the sub–carriers involved in a particular error event since $\boldsymbol{W}_{S_jD}$, $\boldsymbol{W}_{S_jR}$, and $\boldsymbol{W}_{RD}$ depend on the sub–carriers. Since this dependence is cumbersome for optimization, we first find

$$\Phi_Z \ \triangleq \ \min_{\boldsymbol{W}_Z \in \boldsymbol{\mathcal{W}}_Z} \prod_{m=1}^{r_Z} \lambda_m(\boldsymbol{W}_Z \boldsymbol{C}_Z), \tag{35}$$

where $\boldsymbol{\mathcal{W}}_Z$ is the set of all possible matrices $\boldsymbol{W}_Z$, $Z \in \{S_jD, S_jR, RD\}$, $\forall j$. These sets are defined by the sub–carrier allocation at the relays and the interleaver at the source and can be easily determined. Using Φ_Z, $\forall Z$, in (32) implies a further upper bounding of the worst–case PEP.

A. Relay Placement

Consider the location of the nodes in a coordinate system, i.e., $S_1(x_1, y_1)$, $S_2(x_2, y_2)$, …, $S_K(x_K, y_K)$, $R(x_R, y_R)$, and $D(x_D, y_D)$, cf. Fig. 4. Without loss of generality, we assume $x_m \geq 0$ and $y_m \geq 0$, $m \in \{1, 2, \ldots, K, R, D\}$. The distances

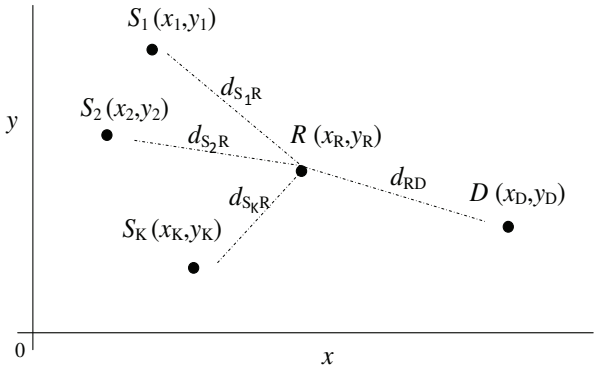

Fig. 4. Schematic diagram of the considered cooperative diversity system for relay placement.

between different nodes are defined as

$$d_{S_jV} \triangleq \sqrt{(x_j - x_V)^2 + (y_j - y_V)^2} \quad \text{and} \quad d_{RD} \triangleq \sqrt{(x_R - x_D)^2 + (y_R - y_D)^2}, \tag{36}$$

where $j \in \{1, 2, \ldots, K\}$ and $V \in \{R, D\}$. Invoking Φ_Z, $\forall Z$, we obtain a relay placement cost function from (32) as

$$J_r^j = \frac{1}{(\xi\bar{\gamma}_{S_jD})^{r_{S_jD}}\Phi_{S_jD}} \times \left[\sum_{l=1}^{K} \frac{\theta_{l,R}^j}{(\xi\bar{\gamma}_{S_lR})^{r_{S_lR}}\Phi_{S_lR}} + \frac{\theta_{RD}^j}{(\xi\bar{\gamma}_{RD})^{r_{RD}}\Phi_{RD}}\right], \tag{37}$$

where all terms not relevant for relay placement have been omitted. To simplify optimization, we note that for $M \geq 8$, we have $\{\varphi^{-(r_{S_jD}+r_{S_lR})}, \varphi^{-(r_{S_jD}+r_{RD})}\} \gg 1$ (e.g., $\varphi = 0.1961$ for 16–QAM with Gray labeling) in (37) which results in $\theta_{l,R}^j \simeq K/(4\varphi^{r_{S_jD}+r_{S_lR}})$ and $\theta_{RD}^j \simeq K/(4\varphi^{r_{S_jD}+r_{RD}})$, $\forall j, l$. With this approximation, we simplify (37) to

$$J_r \simeq \sum_{l=1}^{K} \frac{1}{(\xi\varphi\bar{\gamma}_{S_lR})^{r_{S_lR}}\Phi_{S_lR}} + \frac{1}{(\xi\varphi\bar{\gamma}_{RD})^{r_{RD}}\Phi_{RD}}, \tag{38}$$

which is independent of the $S_j \to D$ link parameters. If the path–loss exponent is assumed to be $\alpha = 2$ and the noise variances at R and D are identical, i.e., $\sigma_Z^2 = d_Z^{-2}$, $Z \in \{S_jD, S_jR, RD\}$, $\forall j$ and $\sigma_{n_{S_jD}}^2 = \sigma_{n_{S_jR}}^2 = \sigma_{n_{RD}}^2 = N_0$, $\forall j$, the cost–function for relay placement based on (36) and (38) can be expressed as

$$J_r \cong \sum_{l=1}^{K} \frac{[(x_l - x_R)^2 + (y_l - y_R)^2]^{r_{S_lR}}}{a_{S_lR}} + \frac{[(x_R - x_D)^2 + (y_R - y_D)^2]^{r_{RD}}}{a_{RD}}, \tag{39}$$

where $a_{S_lR} = (\xi\varphi\bar{\gamma}_l)^{r_{S_lR}}\Phi_{S_lR}$ and $a_{RD} = (\xi\varphi\bar{\gamma}_R)^{r_{RD}}\Phi_{RD}$ with average transmit SNR $\bar{\gamma}_m \triangleq P_m/N_0$, $m \in \{1, \ldots, K, R\}$. For evaluation of the cost function, we assume the destination knows r_U (i.e., L_U) and Φ_U, $U \in \{S_1R, \cdots, S_KR, RD\}$[4]. The optimum relay location is ob-

[4] L_{RD} and Φ_{RD} can be obtained at D based on the estimates for $\boldsymbol{h}_{RD}$, and information about L_{S_lR} and Φ_{S_lR} can be forwarded from R to D via a low rate feedback channel.

tained from

$$\{x_R^\star, y_R^\star\} = \arg \min_{x_R,\ y_R} J_r, \tag{40}$$

$$\text{s.t.} \begin{cases} \min\{x_1, \ldots, x_K, x_D\} \le x_R \le \max\{x_1, \ldots, x_K, x_D\} \\ \min\{y_1, \ldots, y_K, y_D\} \le y_R \le \max\{y_1, \ldots, y_K, y_D\} \end{cases},$$

where the lower and upper limits on x_R and y_R form a rectangular plane where the solution $\{x_R^\star, y_R^\star\}$ lies. The optimization problem in (40) is a standard non–convex polynomial programming problem and a general closed form solution for (40) does not seem to exist. However, this problem can be efficiently solved by Sum of Squares Tools (SOSTools) [24] which are based on semi–definite programming. Below a special case of (40) is discussed where a closed–form solution can be obtained.

Special Case (flat–fading links): Here, $r_{S_jR} = r_{RD} = 1$, $\forall j$, in (39). By calculating $\partial J_r/\partial x_R = 0$ and $\partial J_r/\partial y_R = 0$, and solving for x_R^* and y_R^*, we have

$$x_R^* = \frac{\frac{x_1}{P_1} + \frac{x_2}{P_2} + \ldots + \frac{x_K}{P_K} + \frac{x_R}{P_R}}{\frac{1}{P_1} + \frac{1}{P_2} + \ldots + \frac{1}{P_K} + \frac{1}{P_R}}$$
$$\text{and} \quad y_R^* = \frac{\frac{y_1}{P_1} + \frac{y_2}{P_2} + \ldots + \frac{y_K}{P_K} + \frac{y_R}{P_R}}{\frac{1}{P_1} + \frac{1}{P_2} + \ldots + \frac{1}{P_K} + \frac{1}{P_R}}, \tag{41}$$

and for equal power allocation $P_1 = P_2 = \cdots = P_K = P_R = P_T/(K+1)$ and total transmit power P_T, we have $x_R^* = \frac{x_1+\ldots+x_K+x_D}{K+1}$ and $y_R^* = \frac{y_1+\cdots+y_K+y_D}{K+1}$. For example, if we have one source, the relay should be placed in the middle between the source and the destination. Though not proven analytically, it will be shown in Section V-B that the above choice of x_R^* and y_R^* is close–to–optimal for the general case of equal–diversity channels, i.e., $L_{S_jR} = L_{RD} = L$, $\forall j$.

B. Power Allocation

Another interesting and practical problem is power allocation among transmitting nodes. Based on (32) and (35), we obtain the cost function for power allocation as

$$J_p^j = \frac{1}{(\eta_{S_j,D} P_j)^{r_{S_jD}} \Phi_{S_jD}} \left[\sum_{l=1}^{K} \frac{\theta_{l,R}^j}{(\eta_{S_lR} P_l)^{r_{S_lR}} \Phi_{S_lR}} + \sum_{i=1, i\neq j}^{K} \frac{\theta_{i,D}}{(\eta_{S_i,D} P_i)^{r_{S_iD}} \Phi_{S_iD}} + \frac{\theta_{RD}^j}{(\eta_{RD} P_R)^{r_{RD}} \Phi_{RD}} \right], \tag{42}$$

where $\eta_Z \triangleq \frac{\xi \sigma_Z^2}{N_0}$, $Z \in \{S_jD, S_jR, RD\}$. In the following, we focus on a fair design which aims at minimizing the maximum PEP among all sources. The corresponding optimization problem can be formulated as[5]

$$\min_{P_1,\ldots,P_K,P_R} \quad \max_j \ J_p^j \tag{43}$$
$$\text{s.t.} \begin{cases} P_R + \sum_{j=1}^K P_j \le P_T \\ 0 < P_n \le P_{n,\max}, \quad n \in \{1, \cdots, K, R\} \end{cases}$$

[5]We note that since matrices $\boldsymbol{W}_Z$, $Z \in \{S_jD, S_jR, RD\}$, $\forall j$ in (32) are sub–carrier dependent, performance could be further improved by allocating different powers to different sub–carriers. A corresponding cost function for optimization could be obtained from the union bound over all possible worst–case PEPs within one OFDM symbol. However, this would increase the complexity of the optimization problem considerably.

where P_T and $P_{n,\max}$ denote the total transmit power of all nodes and the maximum transmit power of node n, respectively. Introducing an auxiliary variable Ω, the problem in (43) can be transformed to

$$\min_{\Omega,P_1,\ldots,P_K,P_R} \quad \Omega \tag{44}$$
$$\text{s.t.} \begin{cases} J_p^j \le \Omega, \quad \forall j \\ P_R + \sum_{j=1}^K P_j, \le P_T \\ 0 < P_n \le P_{n,\max}, \quad n \in \{1, \cdots, K, R\}. \end{cases}$$

Since the objective function, J_p^j, and all constraints can be written in the form of posynomials in P_j, $\forall j$, P_R, and Ω, the optimization problem in (44) can be cast into a geometric program (GP) [25], which can be efficiently solved numerically using standard software [26]. We refer to the solution of this problem $\{P_1^*, \ldots, P_K^*, P_R^*\}$ as optimal power allocation (OPA) and compare OPA with equal power allocation (EPA) in Section V.

V. Simulation Results

In this section, we present Monte–Carlo simulation results to investigate the impact of the various system and channel parameters on the performance of network coded cooperative BICM–OFDM. Throughout this section, we adopt the rate $1/2$ convolutional code with generator polynomials $(7,5)_8$ and free distance $d_{\mathrm{f}} = 5$, Gray labeling, and $N_t = 64$ sub–carriers of which $N = 60$ are data sub–carriers, unless stated otherwise. The interleaver for BICM–OFDM is designed as outlined in [15]. The coefficients of each CIR are independent and identically distributed and Rayleigh fading. We assume identical noise variances at R and D, i.e., $\sigma_{n_Z}^2 = N_0$, $Z \in \{S_jD, S_jR, RD\}$, $\forall j$. Note that $\sigma_Z^2 = d_Z^{-\alpha}$ holds and we assume path–loss exponent to be $\alpha = 2$. Unless otherwise mentioned, we assume d_{S_jD} to be normalized to 1, and all other normalized relay link distances are 0.5. As the asymptotic PEP in (32) is obtained via multiple upper bounding steps, we do not show the error rate bounds but validate the derived analytical results in terms of the diversity gain instead. A similar approach was used in [11], [12], [15], [23].

A. Diversity Gain

First, we consider a system with $K = 2$ sources and 16–QAM modulation. We assume equal power allocation at all transmitting nodes, i.e., $P_j = P_R = P$, $\forall j$. Fig. 5 shows the bit error rate (BER) of source S_1 vs. transmit SNR (P/N_0) for different CIR lengths $\{L_{S_1D}, L_{S_2D}, L_{S_1R}, L_{S_2R}, L_{RD}\}$. We consider nine different cases in order to validate the expression for the diversity gain presented in (34): Case 1 {1,1,1,1,1}, Case 2 {2,1,1,1,1}, Case 3 {2,2,1,1,1}, Case 4 {2,1,2,1,2}, Case 5 {2,1,2,2,2}, Case 6 {2,2,2,2,2}, Case 7 {4,2,2,2,2}, Case 8 {5,5,5,5,5}, and Case 9 {6,6,6,6,6}. For Case 1, $G_d^1 = 2$. Cases 2 to 5 all result in $G_d^1 = 3$ which confirms (34). We observe that in Case 5, diversity order G_d^1 for source S_1 is affected by the poor direct link of source S_2 (L_{S_2D} is small compared to frequency diversity of other links). This is expected for network coded BICM–OFDM systems as

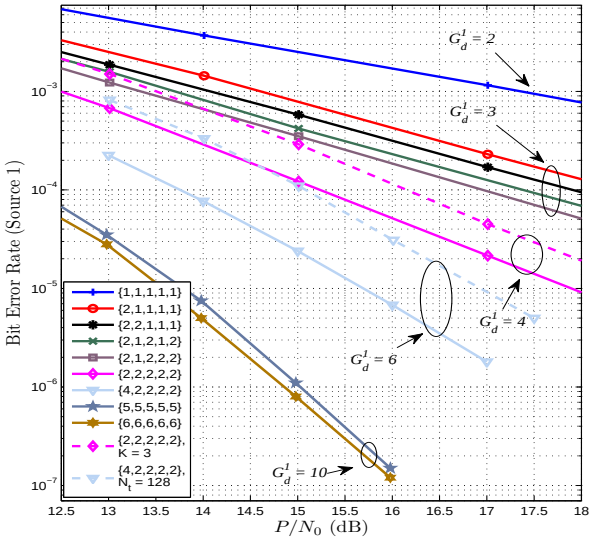

Fig. 5. BER vs. transmit SNR of cooperative network coded BICM–OFDM with one relay and two sources.

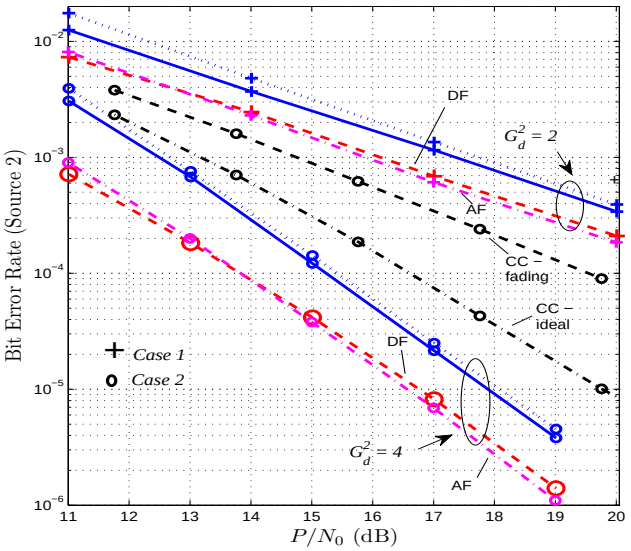

Fig. 6. BER vs. transmit SNR of cooperative network coded BICM–OFDM with one relay and two sources. Solid lines: Full complexity (FC) decoding. Dotted lines: Low complexity (LC) decoding. Results for DF relaying, AF relaying, and coded cooperation (CC) [29] are also shown.

the destination combines the direct link signals received from all sources along with the relayed network coded signal to decode the information transmitted by the sources, and hence the qualities of all links affect the reliability of information transmission by all sources. Though the same diversity order is obtained for Cases 2 to 5, the coding gain increases from Case 2 to Case 5 which can be attributed to the lower correlation between sub–carriers for larger CIR lengths. For Cases 6 and 7, we have $G_d^1 = 4$ and $G_d^1 = 6$, respectively. Furthermore, for Cases 8 and 9, we have $G_d^1 = 10$, as a frequency diversity of the links higher than d_{f} does not contribute to the diversity gain but may improve the coding gain. For Case 6, we also show the BER for $K = 3$ sources and observe that as K increases from two to three, full diversity is maintained but a loss in coding gain results. However, this loss is compensated by the increase in throughput. For Case 7, we also show the BER for an OFDM system with $N_t = 128$ sub–carriers and $N = 120$ data sub–carriers. We observe a coding gain loss of about 1.5 dB as N_t increases from 64 to 128. This loss can be attributed to the increased correlation between sub–carriers when a larger number of sub–carriers is allocated to the same total bandwidth.

TABLE I
COMPLEXITY COMPARISON OF FULL COMPLEXITY (FC) AND LOW COMPLEXITY (LC) DECODING IN TERMS OF TOTAL NUMBER OF METRICS CALCULATED FOR EACH BIT AND LABEL.

Parameters	**Case** 1	**Case** 2	**Case** 3
K	2	2	3
M	4	16	16
# of metric computations: FC	16	256	6144
# of metric computations: LC	10	136	2184

In Fig. 6, we compare the performance of FC and LC decoding for network coded cooperative BICM–OFDM with $K = 2$ sources and 16–QAM modulation. We assume that all nodes transmit with identical powers. We show the BER performance of source S_2 for two different cases: Case 1 $\{L_{S_jD}, L_{S_jR}, L_{RD}\} = \{1, 1, 1\}$, $\forall j$, which yields $G_d^2 = 2$ and Case 2 $\{L_{S_jD}, L_{S_jR}, L_{RD}\} = \{2, 2, 2\}$, $\forall j$, which results in $G_d^2 = 4$. We observe that the LC decoding scheme (dotted lines) performs very close (in the range of 0.1 to 0.5 dB) to the FC implementation (solid lines) for both cases. In Table I, we compare the complexities of FC and LC decoding for three different cases, which clearly reveals that the LC scheme results in significant computational savings as K and/or M increase. Fig. 6 also contains the performance of DF and AF relaying (i.e., cooperative relaying without network coding) which require four orthogonal channels to transmit the signals of two sources. Understandably, DF [22] and AF [21] relaying perform better than network coded relaying but the performance loss of network coded BICM–OFDM is more than compensated by the gain in throughput. Furthermore, for Case 2, we compare the proposed network coded scheme with the coded cooperation (CC) scheme in [29] assuming both schemes consume the same overall power and transmit with the same rate. In CC, two sources transmit to a common destination, where each source tries to decode the other source's transmitted packet and, if successful, transmits additional parity bits for the other source to the destination. Since CC requires only two orthogonal channels whereas the proposed scheme requires three orthogonal channels, we adopt 8–PSK modulation for CC to enable a fair comparison with respect to rate. We consider two scenarios for CC with 50% cooperation [29]: a) an ideal inter–source channel and b) a fading inter–source channel, where the average SNR of the inter–source channel is assumed to be identical to the average

SNR of the source–relay channels for the proposed scheme We observe that CC does not achieve full diversity even with perfect inter–source channel. This loss in diversity is caused by the fact that different bits of an error event may arrive a the destination via different links. For example, let $d_{\mathrm{f}_1}^2$ and $d_{\mathrm{f}_2}^2$ denote the number of erroneous bits of an error even of source S_2 transmitted by sources S_1 and S_2, respectively Then, error events with $d_{\mathrm{f}_1}^2 < L_{S_1D}$ and/or $d_{\mathrm{f}_2}^2 < L_{S_2L}$ dominate the overall performance of CC at high SNR, which limits the diversity gain. For the practically relevant case of a fading inter–source channel, the performance of CC degrades further. In particular, when the CRC detects an error at one o the sources, the sources do not cooperate, which results in a further diversity loss.

Next, in Fig. 7, we compare the performance of conventiona C–MRC decoding based on instantaneous sub–carrier channe gains and LOC–MRC decoding where the average $S_j \to F$ link sub–carrier SNRs are used. We consider a system with two sources and show the BER performance of source S_2. We consider scenarios where the $R \to D$ link is stronger compared to the $S_j \to R$ links such that weight factor $\lambda[k] < 1$ plays a significant role in combining. For this purpose, we set the relay location as $d_{S_1R} = d_{S_2R} = 0.7$ and $d_{RD} = 0.3$ (i.e., the path–loss in the $R \to D$ link is less prominent), where d_{S_1D} and d_{S_2D} are normalized to unity. We show the performance for four different cases: Case 1: QPSK modulation, $\{L_{S_jD}, L_{S_jR}\} = \{1,1\}$, $j \in \{1,2\}$, $L_{RD} = 2$; Case 2: 16-QAM modulation, $\{L_{S_jD}, L_{S_jR}\} = \{1,1\}$, $j \in \{1,2\}$, $L_{RD} = 2$; Case 3: BPSK modulation, $\{L_{S_jD}, L_{S_jR}\} = \{1,1\}$, $j \in \{1,2\}$, $L_{RD} = 4$; Case 4: QPSK modulation, $\{L_{S_1D}, L_{S_jR}\} = \{1,1\}$, $j \in \{1,2\}$, $\{L_{S_2D}, L_{RD}\} = \{2,2\}$. We observe that for Cases 1 to 3, $G_d^2 = 2$ and for Case 4, $G_d^2 = 3$. We notice that LOC–MRC performs very close to C–MRC for all considered cases. At high SNR, the performance gap for different cases lies in the range of 0.1 to 0.3 dB. We also show the performance of conventional MRC for Case 3, which, as outlined in Section II-C, results in a loss of diversity. Furthermore, we see that LOC–MRC combined with LC decoding also achieves high performance (Case 3).

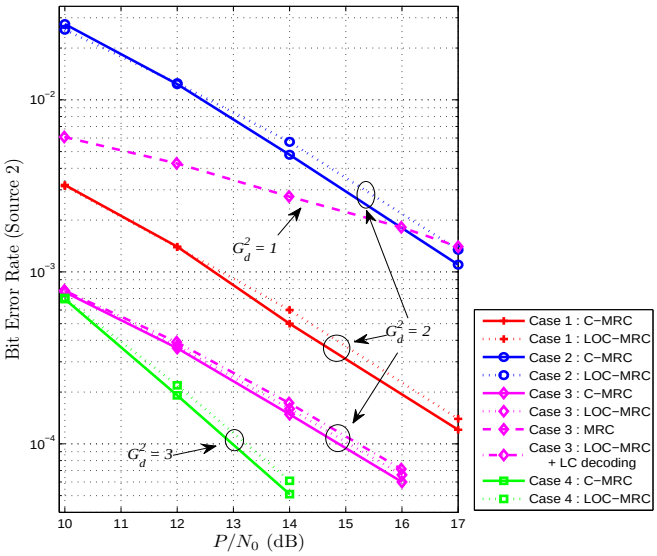

Fig. 7. BER vs. transmit SNR of cooperative network coded BICM–OFDM with one relay and two sources. Solid lines: C–MRC decoding. Dotted lines: LOC–MRC decoding. Dashed lines: MRC decoding. Dashed–dotted lines: LOC–MRC with LC decoding.

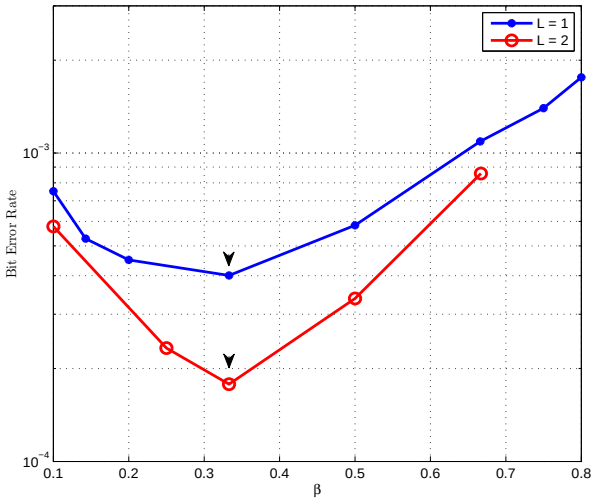

Fig. 8. BER vs. β for one relay and two sources. Equal transmit SNRs and identical frequency diversity L for all links. $x_R = \beta(x_1 + x_2 + x_D)$ and $y_R = \beta(y_1 + y_2 + y_D)$. We assume $S_1(1,1)$, $S_2(1,5)$, and $D(4,3)$. In these cases, we have $x_R^* = 2$ and $y_R^* = 3$ (indicated by pointers) which result for $\beta = 1/3$.

B. Relay Placement

Next, we consider optimal relay placement for a network with two sources and one relay and 16-QAM modulation (cf. Fig. 4). First, we assume identical frequency diversity for all links, i.e., $L_{S_jD} = L_{S_jR} = L_{RD} = L$, $j \in \{1,2\}$, and C–MRC decoding. In Section IV-A, we have shown that for flat–fading links, $x_R^* = \frac{x_1+\ldots+x_K+x_D}{K+1}$ and $y_R^* = \frac{y_1+\cdots+y_K+y_D}{K+1}$ are optimal. In Fig. 8, we examine the BER of source S_1/S_2 (the BERs of both sources are identical since the channel conditions are identical) vs. β, where $x_R = \beta(x_1 + x_2 + x_D)$ and $y_R = \beta(y_1 + y_2 + y_D)$ for $L \in \{1,2\}$. For $L = 1$, $\beta = 1/3$ yields the minimum BER, which is in agreement with $\beta = 1/(K+1)$ as derived in Section IV-A. Interestingly, for $L = 2$, the choice of $\beta = 1/3$ is also optimal. Similar observations have been made for larger values of L as well. Next, in Table II, we study the relay placement problem more in detail. We assume $P_j = P_R = P$, $\forall j$. Four cases are examined for a target transmit SNR of $P/N_0 = 20$ dB. The locations of the sources and the destination are given by $S_1(1,1)$, $S_2(1,5)$, and $D(4,3)$, respectively, in the coordinate system shown in Fig. 4. For source S_1, we compare the performance of optimal relay placement (ORP) with the performance of the solution obtained under the flat–fading assumption (i.e., $x_R^f = (x_1+x_2+x_D)/3 = 2$ and $y_R^f = (y_1+y_2+y_D)/3 = 3$, where f stands for flat fading). For Case 1, we observe that the $R \to D$ link is stronger (L_{RD} is larger) and the relay should be placed closer to the sources ($x_R^* < x_R^f$). If L_{RD} is increased further, we can afford to place the relay even closer to the

TABLE II

RELAY PLACEMENT FOR A SYSTEM WITH TWO SOURCES. RESULTS ARE SHOWN FOR TRANSMIT SNR $P/N_0 = 20$ DB. THE NOISE VARIANCE N_0 IS ASSUMED TO BE IDENTICAL FOR ALL LINKS. WE ASSUME $S_1(1,1)$, $S_2(1,5)$, AND $D(4,3)$. SIMULATED BER RESULTS ARE SHOWN FOR SOURCE S_1.

Parameters	**Case** 1	**Case** 2	**Case** 3	**Case** 4
L_{S_1D}	1	1	1	1
L_{S_2D}	1	1	1	1
L_{S_1R}	1	1	2	3
L_{S_2R}	1	1	2	1
L_{RD}	2	3	1	1
$x_R^\star$	1.64	1.00	2.38	2.50
$y_R^\star$	3.00	3.00	3.00	4.00
Simulated BER (ORP)	4.5×10^{-4}	2.6×10^{-4}	1.178×10^{-4}	1.4×10^{-4}
Simulated BER (flat–fading assumption)	6.8×10^{-4}	3.2×10^{-4}	1.9×10^{-4}	2.0×10^{-4}

TABLE III

POWER ALLOCATED TO SOURCES S_1, S_2, AND RELAY R. WE ASSUME $d_{S_jR} = 1 - d_{RD}$, $d_{S_jD} = 1$, $j \in \{1,2\}$, AND $P_T = 3$. RESULTS ARE SHOWN FOR $P_T/N_0 = 25$ DB. THE NOISE VARIANCE N_0 IS ASSUMED TO BE IDENTICAL FOR ALL LINKS. BER RESULTS ARE OBTAINED VIA SIMULATION.

Parameters	**Case** 1	**Case** 2	**Case** 3	**Case** 4
d_{RD}	0.5	0.75	0.3	0.5
L_{S_1D}	2	1	1	1
L_{S_2D}	1	1	1	1
L_{S_1R}	1	1	1	1
L_{S_2R}	1	1	1	1
L_{RD}	1	1	2	1
$P_1^\star$	0.8934	1.0	1.3624	1.1877
$P_2^\star$	1.5132	1.0	1.3624	1.1877
$P_R^\star$	0.5934	1.0	0.2752	0.6244
BER (OPA), S_1	4.14×10^{-7}	2.59×10^{-5}	2.82×10^{-5}	1.41×10^{-5}
BER (EPA), S_1	3.56×10^{-7}	2.59×10^{-5}	4.22×10^{-5}	2.06×10^{-5}
BER (OPA), S_2	1.20×10^{-5}	2.59×10^{-5}	2.82×10^{-5}	1.41×10^{-5}
BER (EPA), S_2	3.48×10^{-5}	2.59×10^{-5}	4.22×10^{-5}	2.06×10^{-5}

sources (Case 2). On the other hand, if the $S_j \to R$ links are stronger, the relay should be placed closer to the destination ($x_R^* > x_R^f$) to compensate for the poor $R \to D$ link (Case 3). Note that for Cases 1 to 3, symmetric frequency diversity links (i.e., $L_{S_1D} = L_{S_2D}$ and $L_{S_1R} = L_{S_2R}$) are assumed, hence the choice of $y_R^* = y_R^f = 3$ has not changed. In Case 4, we assume an asymmetric scenario and set $L_{S_1D} = 3$, i.e., the $S_1 \to D$ link has the highest frequency diversity among all links. As the $S_1 \to R$ link is stronger, the relay should be placed relatively closer to S_2 and D, as reflected by the choices of $x_R^* = 2.5 > x_R^f$ and $y_R^* = 4.0 > y_R^f$. In all cases, we observe that ORP achieves a better performance compared to the choice based on the flat–fading assumption.

C. Power Allocation

In Fig. 9, we show the frame error rate (FER) of sources S_1 and S_2 as a function of P_T/N_0 for the considered cooperative diversity system with two sources and one relay, QPSK modulation, and C–MRC decoding. For the following, we assume $P_{j,\max} = P_{R,\max} = 0.95P_T$ and $P_T = 3$. In Fig. 9, we compare EPA and OPA (cf. (44)) for $L_{S_1D} = 2$, $L_{S_2D} = L_{S_jR} = L_{RD} = 1$, $j \in \{1,2\}$, and $d_Z = 1$. We observe that source S_1 enjoys better link qualities for the considered scenario compared to source S_2. To achieve fairness, OPA ($P_1^* = 0.8158, P_2^* = 1.5880, P_R^* = 0.5962$) allocates more power to S_2 compared to S_1 and R. At FER = 4×10^{-4}, we observe that the performance of S_2 improves by 1.5 dB, whereas the performance of S_1 degrades slightly (by 0.5 dB) compared to the performance achieved by EPA. To gain more insight, we investigate the impact of the link quality (i.e., path loss and frequency diversity) on power allocation in Table III. If the relay is placed at equal distance from the sources and the destination and the $S_1 \to D$ link is stronger (larger L_{S_1D}), then S_2 is allocated more power compared to S_1 as it has weaker links, and thus OPA injects fairness into the system (Case 1). If the frequency diversities of all links are identical and the relay is placed closer to the sources, then to compensate for the poor $R \to D$ link, more power is allocated to the relay (Case 2). In Case 2, we find that EPA is optimum. On the other hand, if the $R \to D$ link is stronger (higher L_{RD} and lower path–loss), very little power is allocated to the relay, and the two sources receive most

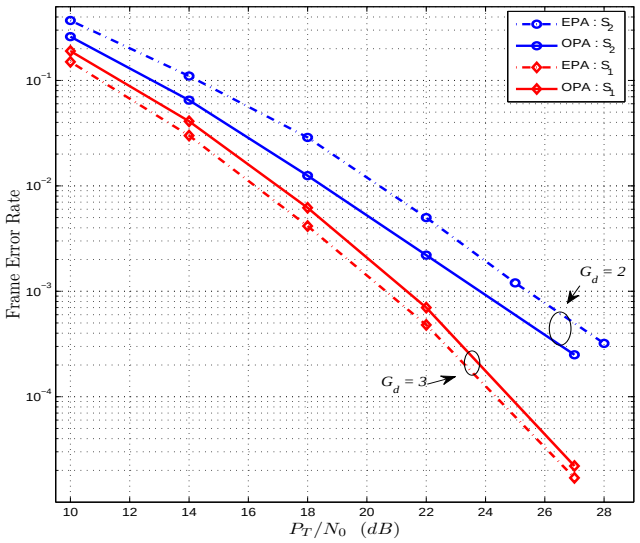

Fig. 9. FER vs. P_T/N_0 of the considered network coded cooperative BICM–OFDM for different power allocation schemes. Solid lines: Equal power allocation (EPA). Dashed lines: Optimum power allocation (OPA).

of the share of the total power, cf. Case 3. Finally, in Case 4, where the relay is placed at equal distance from the two sources and the destination and all links are flat–fading, most of the available power is given to the sources. For all cases, we observe that OPA performs better than EPA in terms of BER, showing the merits of the proposed power allocation scheme.

VI. Conclusions

In this paper, we studied multi–source cooperative BICM–OFDM systems employing GF(2) network coding and proposed a generalized C–MRC bit metric for decoding at the destination, which achieves the maximum possible diversity of the considered system even if erroneous decisions at the relay are taken into account. Furthermore, we introduced a **new** (low feedback overhead) LOC–MRC bit metric and a low complexity decoding scheme, which both perform close to C–MRC with full complexity decoding. We derived closed–form expressions for an upper bound on the asymptotic PEP and the diversity order of the system for C–MRC decoding. The diversity analysis revealed that, unlike for AF and DF relaying, the diversity order of a particular source in a network coded BICM–OFDM system may be limited by the frequency diversity of the source–destination links of the other sources. The results from the PEP analysis were exploited for formulating optimization problems for relay placement and power allocation, which can be solved using polynomial and geometric programming techniques, respectively. For relay placement, we found that the closed–form solution obtained for flat fading is also close–to–optimum for the frequency–selective case with equal–diversity links. For power allocation, we observed that, unless the $R \to D$ link is very poor, the sources receive a larger share of the power than the relay.

References

[1] J. N. Laneman, D. N. C. Tse, and G. W. Wornell. Cooperative Diversity in Wireless Networks: Efficient Protocols and Outage Behavior. *IEEE Trans. Inform. Theory*, 50:3062–3080, September 2004.

[2] A. Nosratinia, T. Hunter, and A. Hedayat. Cooperative Communication in Wireless Networks. *IEEE Commun. Mag.*, 42:68–73, October 2004.

[3] A. Sendonaris, E. Erkip, and B. Aazhang. User Cooperation Diversity – Parts I and II. *IEEE Trans. Commun.*, 51:1927–1948, November 2003.

[4] J.N. Laneman and G.W. Wornell. Distributed Space–Time Block Coded Protocols for Exploiting Cooperative Diversity in Wireless Networks. *IEEE Trans. Inform. Theory*, 49:2415–2425, October 2003.

[5] A. Ribeiro, X. Cai, and G.B. Giannakis. Opportunistic Multipath for Bandwidth–Efficient Cooperative Networking. In *Proceedings of IEEE Int. Conf. on Acou., Speech, and Signal Process.'04*, Montreal, Canada, May 2004.

[6] R. Ahlswede, N. Cai, S. Li, and R. Yeung. Network Information Flow. *IEEE Trans. Inform. Theory*, 46:1204–1216, July 2000.

[7] Y. Chen, S. Kishore, and J. Li. Wireless Diversity Through Network Coding. In *Proceedings of IEEE Wireless Commun. and Network. Conf.'06*, Las Vegas, NV, April 2006.

[8] M. Yu, J. Li, and R. Blum. User Cooperation Through Network Coding. In *Proceedings of IEEE Int. Conf. Commun.'07*, Glasgow, Scotland, June 2007.

[9] L. Xiao, Jr. D. Costello, and T. Fuja. Network Coded Cooperative Diversity with Multiple Sources. In *Proceedings of IEEE Global Commun. Conf.'09*, Honolulu, HI, December 2009.

[10] S. Zhang, S. Liew, and P. Lam. Hot Topic: Physical Layer Network Coding. In *Proceedings of Int. Conf. Mobile Comp. and Network.'06*, Los Angeles, CA, September 2006.

[11] T. Wang and G. Giannakis. Complex Field Network Coding for Multiuser Cooperative Communications. *IEEE J. Select. Areas Commun.*, 26:561–571, April 2008.

[12] A. Cano, T. Wang, A. Ribeiro, and G. Giannakis. Link–Adaptive Distributed Coding for Multi–Source Cooperation. *EURASIP Journal on Adv. in Signal Process.*, 2008:1–12, January 2008.

[13] D. H. Woldegebreal and H. Karl. Multiple–Access Relay Channel with Network Coding and Non–Ideal Source–Relay Channels. In *International Symposium on Wireless Communication Systems (ISWCS)'07*, Trondheim, December 2007.

[14] A. Nasri, R. Schober, and M. Uysal. Error Rate Performance of Network–coded Cooperative Diversity Systems. In *Proceedings of IEEE Global Commun. Conf.'10*, Miami, FL, December 2010.

[15] E. Akay and E. Ayanoglu. Achieving Full Frequency and Space Diversity in Wireless Systems via BICM, OFDM, STBC, and Viterbi Decoding. *IEEE Trans. Commun.*, 54:2164–2172, December 2006.

[16] S. Nguyen, A. Ghrayeb, G. Al-Habian, and M. Hasna. Mitigating Error Propagation in Two-Way Relay Channels with Network Coding. *IEEE Trans. Wireless Commun.*, 9:3380–3390, November 2010.

[17] S. Zhang and S. Liew. Channel Coding and Decoding in a Relay System Operated with Physical-Layer Network Coding. *IEEE J. Select. Areas Commun.*, 27:788–796, June 2009.

[18] X. Xu, Y. Jing, X. Yu. Subspace–based Noise Variance and SNR Estimation for OFDM Systems. In *Proceedings of IEEE Wireless Commun. and Network. Conf.' 05*, Los Angeles, USA, March 2005.

[19] A. Zhan, C. He, and L. Jiang. A Turbo–BICM based scheme for joint Network Coding and Channel Coding. In *Proc. IEEE Int. Conf. Commun.'10*, Cape Town, South Africa, May 2010.

[20] H. Gacanin and F. Adachi. Broadband Analog Network Coding. *IEEE Trans. Wireless Commun.*, 9:1577–1583, May 2010.

[21] T. Islam, R. Schober, R. K. Mallik, and V. K. Bhargava. Analysis and Design of Cooperative BICM–OFDM Systems. *IEEE Trans. Commun.*, 59:1742– 1751, June 2011.

[22] T. Islam, A. Nasri, R. Schober, and R. K. Mallik. Analysis and Relay Placement for DF Cooperative BICM–OFDM Systems. In *Proceedings of IEEE Wireless Commun. and Network. Conf.'11*, Cancun, Mexico, March 2011.

[23] T. Wang, A. Cano, G. B. Giannakis, and J. N. Laneman. High-Performance Cooperative Demodulation with Decode-and-Forward Relays. *IEEE Trans. Commun.*, 55:1427– 1438, July 2007.

[24] S. Prajna, A. Papachristodoulou, P. Seiler, and P. A. Parrilo. *SOSTOOLS: Sum of squares optimization toolbox for MATLAB*, 2004.

[25] S. Boyd and L. Vandenberghe. *Convex Optimization*. Cambridge Univ. Press, Cambridge, U.K., 2004.

[26] *GGPLAB: A Simple Matlab Toolbox for Geometric Programming. [Online]: http://www.stanford.edu/˜boyd/ggplab/.*

[27] G. Caire, G. Taricco, and E. Biglieri. Bit–Interleaved Coded Modulation. *IEEE Trans. Inform. Theory*, 44:927–946, May 1998.

[28] T. Wang, G. Giannakis, and R. Wang. Smart Regenerative Relays for Link-Adaptive Cooperative Communications. *IEEE Trans. Commun.*, 56:1950–1960, November 2008.

[29] T. Hunter and A. Nosratinia. Diversity Through Coded Cooperation. *IEEE Trans. Wireless Commun.*, 5:283–289, February 2006.

Toufiqul Islam (S'10) received his B.Sc. and M.Sc. degrees in Electrical and Electronic Engineering from Bangladesh University of Engineering and Technology, Dhaka, Bangladesh, in 2006 and 2008, respectively. Currently, he is working toward Ph.D. degree in Electrical and Computer Engineering at The University of British Columbia (UBC), Vancouver, Canada.

His research interests include cooperative communication, wireless network coding, energy efficient networks, and OFDMA cellular networks. He has won the Donald N. Byers Prize, the highest graduate student honor at UBC. He was also the recipient of the prestigious Vanier Canada Graduate Scholarship, Killam Doctoral Fellowship, and UBC Four Year Fellowship in 2011, 2010, and 2009, respectively. His paper was awarded 2nd prize in the IEEE Region 10 undergraduate student paper contest in 2006.

Amir Nasri (S'06, M'08) received the B.S. degree from Sharif University of Technology, Tehran, Iran, in 2001, the M.Sc. degree from University of Tehran, Tehran, Iran, in 2004, and the Ph.D. degree from the University of British Columbia, Vancouver, Canada, in 2008, all in electrical engineering. His current research interests are in the broad areas of performance analysis and optimization of wireless communication systems.

He received the Best Paper Award at the IEEE International Conference on Ultra-Wideband (ICUWB) 2006, and was finalist for the best paper award at 2006 IEEE Global Telecommunications Conference (Globecom 2006). He was also the recipient of the 2007 Li Tze Fong UGF Award from University of British Columbia and the Natural Sciences and Engineering Research Council of Canada (NSERC) postdoctoral fellowship.

Robert Schober (M'01, SM'08, F'10) was born in Neuendettelsau, Germany, in 1971. He received the Diplom (Univ.) and the Ph.D. degrees in electrical engineering from the University of Erlangen-Nuermberg in 1997 and 2000, respectively. From May 2001 to April 2002 he was a Postdoctoral Fellow at the University of Toronto, Canada, sponsored by the German Academic Exchange Service (DAAD). Since May 2002 he has been with the University of British Columbia (UBC), Vancouver, Canada, where he is now a Full Professor and Canada Research Chair (Tier II) in Wireless Communications. His research interests fall into the broad areas of Communication Theory, Wireless Communications, and Statistical Signal Processing.

Dr. Schober received the 2002 Heinz MaierVLeibnitz Award of the German Science Foundation (DFG), the 2004 Innovations Award of the Vodafone Foundation for Research in Mobile Communications, the 2006 UBC Killam Research Prize, the 2007 Wilhelm Friedrich Bessel Research Award of the Alexander von Humboldt Foundation, and the 2008 Charles McDowell Award for Excellence in Research from UBC. In addition, he received best paper awards from the German Information Technology Society (ITG), the European Association for Signal, Speech and Image Processing (EURASIP), IEEE ICUWB 2006, the International Zurich Seminar on Broadband Communications, and European Wireless 2000. Since January 2012, Dr. Schober is serving as the Editor–in–Chief for the IEEE TRANSACTIONS ON COMMUNICATIONS.

Ranjan K. Mallik (M'93, SM'02) received the B.Tech. degree from the Indian Institute of Technology, Kanpur, in 1987 and the M.S. and Ph.D. degrees from the University of Southern California, Los Angeles, in 1988 and 1992, respectively, all in Electrical Engineering. From August 1992 to November 1994, he was a scientist at the Defence Electronics Research Laboratory, Hyderabad, India, working on missile and EW projects. From November 1994 to January 1996, he was a faculty member of the Department of Electronics and Electrical Communication Engineering, Indian Institute of Technology, Kharagpur. From January 1996 to December 1998, he was with the faculty of the Department of Electronics and Communication Engineering, Indian Institute of Technology, Guwahati. Since December 1998, he has been with the faculty of the Department of Electrical Engineering, Indian Institute of Technology, Delhi, where he is currently a Professor. His research interests are in diversity combining and channel modeling for wireless communications, space-time systems, cooperative communications, multiple-access systems, difference equations, and linear algebra.

Dr. Mallik is a member of Eta Kappa Nu. He is also a member of the IEEE Communications, Information Theory, and Vehicular Technology Societies, the American Mathematical Society, and the International Linear Algebra Society, a fellow of the Indian National Academy of Engineering, the Indian National Science Academy, The National Academy of Sciences, India, Allahabad, The Institution of Engineering and Technology, U.K., and The Institution of Electronics and Telecommunication Engineers, India, a life member of the Indian Society for Technical Education, and an associate member of The Institution of Engineers (India). He is an Area Editor for the IEEE TRANSACTIONS ON WIRELESS COMMUNICATIONS and an Editor for the IEEE TRANSACTIONS ON COMMUNICATIONS. He is a recipient of the Hari Om Ashram Prerit Dr. Vikram Sarabhai Research Award in the field of Electronics, Telematics, Informatics, and Automation, and of the Shanti Swarup Bhatnagar Prize in Engineering Sciences.

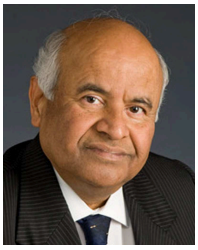

Vijay K. Bhargava (M'74, SM'82, F'92) received his B.Sc., M.Sc., and Ph.D. degrees from Queens University, Kingston, Ontario in 1970, 1972, and 1974, respectively. Vijay has held regular/visiting appointments at the Indian Institute of Science, University of Waterloo, Concordia University, Ecole Polytechnique de Montreal, UNIDO, NTT Wireless Communications Labs, Tokyo Institute of Technology, University of Indonesia, the Hong Kong University of Science and Technology, The Hong Kong University, and the University of Victoria. Currently he is a professor at the Department of Electrical and Computer Engineering at the University of British Columbia. Vijay served as the Founder and President of Binary Communications Inc. (1983-2000). He is a co-author (with D. Haccoun, R. Matyas, and P. Nuspl) of Digital Communications by Satellite (New York: Wiley, 1981); a co-editor (with S. Wicker) of Reed Solomon Codes and their Applications (IEEE Press, 1994); co-editor (with V. Poor, V. Tarokh, and S. Yoon) of Communications, Information and Network Security (Kluwer, 2003); and a co-editor (with E. Hossain) of Cognitive Wireless Communication Networks (Springer, 2007). He has served as the Editor-in-Chief of the IEEE TRANSACTIONS ON WIRELESS COMMUNICATIONS and Editor for the IEEE TRANSACTIONS ON COMMUNICATIONS. He is currently the Director of Journals of the Transactions Editorial Board, IEEE Communications Society. A Fellow of the IEEE, the Engineering Institute of Canada (EIC), the Royal Society of Canada, and the Canadian Academy of Engineering, Vijay has been honoured many times by his colleagues and has received numerous awards. Vijay is very active in the IEEE and has served as the President of the Information Theory Society, Vice President for Regional Activities Board, Director of Region 7, Montreal Section Chair and Victoria Section Chair. He is a past member of the Board of Governors of the IEEE Communications Society. He was nominated by the IEEE BoD as a candidate for the office of President-Elect in 1996, 2002 and 2003. In the recently conducted election of the IEEE Communications Society, Vijay was elected to serve as its President-Elect during 2011 and as President during 2012 and 2013. His current research interests include green communications, cognitive and cooperative wireless systems, MIMO-OFDM systems, and cross-layer analysis.